Copy 6
RM E55K18

NACA RM E55K18

NACA

RESEARCH MEMORANDUM

TEMPERATURE DROPS THROUGH LIQUID-COOLED TURBINE BLADES WITH VARIOUS COOLING-PASSAGE GEOMETRIES

By Edward R. Bartoo

Lewis Flight Propulsion Laboratory
Cleveland, Ohio

NATIONAL ADVISORY COMMITTEE
FOR AERONAUTICS

WASHINGTON

March 23, 1956

NACA RM E55K18

NATIONAL ADVISORY COMMITTEE FOR AERONAUTICS

RESEARCH MEMORANDUM

TEMPERATURE DROPS THROUGH LIQUID-COOLED TURBINE BLADES WITH VARIOUS COOLING-PASSAGE GEOMETRIES

By Edward R. Bartoo

SUMMARY

The effects of variations in cooling-passage geometry on the relations between heat flow and temperature drops within liquid-cooled turbine blades were determined quantitatively. Wall thicknesses, blade section depths, and cooling-passage sizes, shapes, and spacings were varied experimentally on a simple electric analog on which were simulated rectangular sections of blades. Data were obtained for sections heated along one surface and cooled by a row of passages at various distances from that surface. These data were extended to apply to sections heated along two opposing surfaces and cooled by a single row of passages equidistant from those surfaces. Results are presented in terms of the temperature differences between the cooled-surface temperature and (1) the average heated-surface temperature, (2) the minimum heated-surface temperature, (3) the maximum heated-surface temperature, and (4) the maximum temperature at the centerline of the turbine blades.

INTRODUCTION

For some applications of gas-turbine engines, liquid-cooling of the turbine is desirable in order to permit operation at gas-temperature levels higher than is presently feasible. Because of the very high heat-transfer rates possible with liquid-cooling, temperature gradients within the turbine blades can become excessive unless proper design procedures are used. Data presented herein can be used to evaluate temperature differences within liquid-cooled turbine blades for a wide variety of coolant-passage configurations.

Early investigators in the turbine-cooling field realized almost immediately that liquids would provide much stronger cooling than air. Initial liquid-cooling investigations were made to demonstrate this fact and to determine the magnitude of the heat-transfer coefficients that could be realized. Since it was convenient and adequate for the initial investigations and since its properties are well-defined over a wide range

of conditions, water was chosen as the cooling medium. Fabrication problems led to the use of relatively large coolant passages in the turbine blades. Stress considerations required that such passages be of circular cross section in order to better withstand the high coolant pressures developed by centrifugal action at high speeds.

This early research in the field confirmed the expectations for liquid-cooling and provided background for subsequent work. (Refs. 1 and 2 are typical.) In addition, it emphasized some of the problems to be encountered in the further development of liquid-cooled systems for aircraft turbines. Without pressurization, the boiling point of water is low and the maximum coolant temperature within the system is limited. Consequently, turbine blades are overcooled, heat-rejection rates become excessive, and, as shown by reference 3, heat rejection to ambient air at flight Mach numbers above 1.8 is almost impossible with a simple heat exchanger. References 4 and 5 show that the type of cooling passages considered would result in excessive temperature gradients within the turbine blades.

These factors naturally lead to the consideration of cooling systems designed for (1) maximum permissible blade temperatures in order to keep the heat load on the system to a minimum, (2) maximum feasible coolant temperatures in order to facilitate heat rejection to the surrounding atmosphere, and (3) minimum thermal gradients within the blade in order to minimize thermal stresses. Current efforts are being directed toward liquid-metal coolants and the use of small coolant passages closely spaced around the periphery of the turbine blade.

Natural convection governs the circulation of coolants within the rotating parts of liquid-filled cooling systems. Coolant temperature levels have an important bearing on coolant properties and hence on natural-convection circulation. The temperature drop through the turbine blade, if sufficiently large, may have to be accounted for in evaluating coolant circulation and system operation. Heretofore, it has been customary to assume nominal values for such temperature drops or to evaluate them either by numerical methods as discussed in reference 4, or by the use of simple electric analogs as outlined in reference 5. As design procedures are refined and blades and systems are designed nearer their temperature limits, the need for comparative information on the temperature drops through turbine blades with a wide variety of cooling-passage configurations will become increasingly important to the designer.

The present report may be used to obtain an initial survey of a wide range of passage geometries in order to permit the selection of a given configuration (or configurations) best suited to the conditions of operation. Then, if desired, a more accurate and detailed picture of the temperature distribution may be obtained either by applying the methods of reference 4 or by making an analog (or analogs) for the entire blade (or

blades). Data are presented in terms of the differences between the cooled-surface temperature and (1) the average heated-surface temperature, (2) the minimum heated-surface temperature, (3) the maximum heated-surface temperature, and (4) the maximum temperature at the rear of the blade section corresponding to the centerline of the turbine blade. The differences based on average heated-surface temperature are useful for heat-flow calculations; those based on minimum heated-surface temperature permit evaluation of maximum temperature gradients; those based on maximum heated-surface temperatures allow calculation of maximum metal temperatures; and those based on the maximum temperatures at the extreme rear of the blade sections yield the maximum temperature at the centerline of the turbine blade.

With the use of coolant passages of relatively small cross section, the stress problems due to high coolant pressures are not so critical. Consequently, square, rectangular, and/or oval passages may prove feasible for many applications, depending on the fabrication techniques employed. Square, rectangular, and circular passages were investigated herein to permit reasonable approximations of a wide variety of shapes. Data are presented for a range of geometries for each of these cross sections.

SYMBOLS

A area, sq ft

a dimension of cooling passage parallel to surface (fig. 1(b)), in.

b dimension of cooling passage perpendicular to surface (fig. 1(b)), in.

Δe potential difference, v

h heat-transfer coefficient, Btu/(hr)(sq in. or sq ft)($^{\circ}$F)

i current, amp

k thermal conductivity, Btu/(hr)(in. or ft)($^{\circ}$F)

L dimension perpendicular to plane of grid of a metal block whose thermal resistance is represented by a 1-inch length of wire on analog grid (fig. 1(d)), in.

l width of metal block whose thermal resistance is represented by a 1-inch length of wire on the analog grid (fig. 1(d)), in.

n direction normal to surface

[redacted]

Q	heat-flow rate, Btu/hr
Q'	heat-flow rate per square inch of surface area, Btu/(hr)(sq in.)
R_E	electrical resistance, ohms
R_{th}	thermal resistance, (hr)($^\circ$F)/Btu
R'_{th}	thermal resistance per unit surface area, (hr)($^\circ$F)/(Btu)(sq in.)
R_w	unit electrical resistance of analog grid, ohms
T	temperature, $^\circ$F
$\overline{T}$	mean temperature, $^\circ$F
$T_{g,e}$	effective gas temperature, $^\circ$F
ΔT	temperature difference, $^\circ$F
$\overline{\Delta T}$	difference between mean heated-surface temperature and cooled-surface temperature, $^\circ$F
ΔT_{max}	difference between maximum heated-surface temperature and cooled-surface temperature, $^\circ$F
ΔT_{min}	difference between minimum heated-surface temperature and cooled-surface temperature, $^\circ$F
ΔT_r	difference between maximum temperature at rear of simulated blade section (camber line of blade) and cooled-surface temperature, $^\circ$F
t	thickness of metal block whose thermal resistance is represented by a 1-inch length of wire on analog grid, in.
x,y,z	distances along mutually perpendicular axes, ft
Φ	temperature-difference ratio, $(T - T_2)/(T_1 - T_2)$

Subscripts:

o	heated surface
pw	plane wall
1,2	used to distinguish between areas and temperatures on different surfaces of a body

[redacted]

APPARATUS

Thermal resistances of rectangular sections of cooled turbine blades with various cooling-passage configurations were determined from measured electrical resistances of simulated configurations on a resistance analog. Figure 1(a) indicates some typical sections of liquid-cooled blades whose heat-flow paths may be approximated on a simple rectangular analog. An idealized representation of one such blade section is shown in figure 1(b). A uniform heat-transfer coefficient is assumed over one boundary of the section, while no heat flow occurs across the other three sides. A uniform temperature is assumed for all cooling-passage surfaces. The electric analog on which such sections were approximated experimentally is illustrated schematically in figure 1(c). The turbine blade metal was represented by a grid of resistance wire, each length of wire between the welded junctions representing a block of metal as indicated in figure 1(d). Cooling passages were simulated by shorting out appropriate portions of the grid at desired locations (assuming a uniform cooled-surface temperature), and the thermal resistance of the boundary layer on the heated surface of the blade was represented by a series of resistances connected to the wires along one side of the grid (see fig. 1(c)). (The principles and the design of the analog are given in the appendix.)

The wire grid was a 20- by 20-inch square of 1- by 1-inch mesh of 24-gage chromel wire electrically spot-welded at each junction. Wires were held in grooves in a copper template during welding to ensure dimensional accuracy. Varying lengths of 3/16- by 1/4-inch copper bars were used to short out areas of the grid to simulate square and rectangular passages; 11-gage copper wire was used for circular holes. The desired passage shape and size were outlined by copper bars (or wire) which were then clamped in place by heavier copper bars (1/4 by 1 in.). Machine screws projecting up through the grid at intervals from a plywood base facilitated the clamping. The cooling-passage array was connected to the 1/4- by 1-inch copper bus bar adjacent to the grid (fig. 1(c)) by copper bars of the same size. The large bar sizes were used to avoid appreciable voltage drops between coolant passages. Boundaries were set within 1/64 inch for the square and rectangular passages, which were outlined by bars of rectangular cross section, and within 1/32 inch for the circular passages, where wire of circular cross section was used.

The external resistances representing the thermal resistance of the boundary layer at the outer surface of the blade were lengths of calibrated 28-gage chromel wire. Twenty such lengths were welded to the grid at 1-inch intervals along one side, the connections being made 1/2 inch from the grid-wire junctions (fig. 1(c)). The opposite ends of these external resistances were welded to a length of chromel rod that was brazed to a heavy copper bus bar to ensure a uniform electrical potential at these points. The external resistances were initially chosen to correspond to a heat-transfer coefficient of 250 Btu/(hr)(sq ft)($^{\circ}$F) [1.736 Btu/(hr)(sq in.)($^{\circ}$F)] and later for one-fourth that value. (Details are given in the appendix.)

[redacted]

A 6-volt automobile battery and a voltage divider supplied current to the analog. The entire assembly except the battery was mounted on a plywood base.

EXPERIMENTAL PROCEDURE

Once a given passage size, passage shape, passage spacing, and wall thickness had been selected and the corresponding areas of the grid shorted out as indicated in figure 1(c), a potential was applied across the bus bars of the analog. The voltage was adjusted to give a large deflection on the scale of the d-c ammeter which measured current flow. The potential difference between the coolant-passage bus bar and the grid wires within the shorted-out passage areas was checked with a commercial laboratory potentiometer. Any measurable potential difference indicated a poor electrical connection somewhere in that portion of the circuit; such connections were ascertained and the difficulty eliminated. Potential differences were then checked between the cooling-passage bus bar and the 20 points along the edge of the grid which represented the surface of the blade section and also between the cooling-passage bus bar and a point on the extreme rear of the grid midway between cooling passages. 3883

Measurements were taken with various combinations of passage sizes, shapes, and spacings, and with varying wall thicknesses on the full 20-inch-deep grid. It was expected that this grid depth would be sufficiently large with respect to passage dimensions to approximate the condition of infinite grid depth. Subsequently, the grid depth was decreased in a series of steps by cutting off strips from the rear of the grid. At each step the foregoing procedure was repeated for a range of cooling-passage configurations.

Table I indicates the range of conditions for which data are presented.

CALCULATION PROCEDURE

Calculation procedures employed herein involve evaluation of analog electrical resistances for various simulated cooling-passage configurations, determination of the corresponding thermal resistances, and calculation of unit values of $k\Delta T/Q'$ based on a common heated-surface area in order that results may be compared directly. Unit values of $k\Delta T/Q'$ are presented in terms of four different temperature drops to permit ready calculation of the average, minimum, and maximum heated-surface temperatures, and the maximum temperature at the rear boundary of the blade section (table I).

Determination of Thermal Resistance

The electrical resistance of the simulated cooling configuration was first determined from measured analog values of current and voltage drops. The potential differences between the 20 points representing the blade surface and the cooling-passage bus bar were averaged arithmetically. The mean value divided by the measured current gave the electrical resistance for the simulated configuration. This resistance multiplied by the previously determined ratio of thermal to electrical resistance (see appendix) gave the thermal resistance of the configuration.

Thermal resistances based on the minimum and also on the maximum temperature on the heated surface of the simulated blade section were obtained in the same way, except that the minimum and the maximum rather than the average potential drop from the surface to the cooling passage were used in determining the electrical resistances. Similarly, procedures used in evaluating thermal resistances based on the maximum temperature at the rear of the simulated blade section were identical except for the potential difference employed.

Determination of Unit Thermal Resistance

The surface area represented on the analog was $20\ell L$, where ℓ was the width and L the dimension perpendicular to the plane of the grid of the block of metal whose thermal resistance was represented by the electrical resistance of 1 inch of grid wire. The value of L was assumed to be 1 inch at all times, while various values were assumed for the equivalent grid spacing ℓ. The surface area varied with ℓ; and, in order to put results on the basis of a common surface area, the following relation was used:

$$R'_{th} = \frac{\Delta e}{i} \times \frac{R_{th}}{R_E} \times \frac{\text{equivalent analog surface area}}{\text{common reference surface area}}$$

$$= \frac{\Delta e}{i} \times \frac{R_{th}}{R_E} \times \frac{20\ell L}{\text{common surface area}} \qquad (1)$$

where R'_{th} is the thermal resistance per square inch of surface area. In the present case the values assumed (see appendix) reduced equation (1) to

$$R'_{th} = 181\ \ell \frac{\Delta e}{i}, \frac{(hr)(^\circ F)}{Btu} \qquad (2)$$

[redacted]

By assuming different values for the equivalent grid spacing l, the measured electrical resistance for any simulated cooling configuration may be used to obtain thermal resistances for a series of geometrically similar configurations. All physical dimensions of the configuration except L vary directly with l; this includes the surface area, since the dimension perpendicular to the plane of the grid L was assumed 1 inch at all times. Thus, the measured electrical resistance of an analog set up for passages 2×2 grid spaces square spaced 10 grid spaces apart with a wall thickness of 4 grid spaces may be used to evaluate the thermal resistances of (a) 0.010- by 0.010-inch passages spaced 0.050 inch apart with a wall thickness of 0.020 inch, (b) 0.040- by 0.040-inch passages spaced 0.200 inch apart with a wall of 0.080 inch, or (c) any other geometrically similar arrangement.

Justification of the procedure within the limits used herein lies in the fact that a fourfold change in the parameter $h_o t/k$ in the current series of experiments resulted in a spread of only 6 percent in observed data. The analog was originally set up for an outside heat-transfer coefficient of 1.736 Btu/(hr)(sq in.)(°F)[250 Btu/(hr)(sq ft)(°F)], a conductivity of 1.25 Btu/(hr)(in.)(°F)[15 Btu/(hr)(ft)(°F)], and an equivalent grid spacing of 0.005 inch, which gave a value of 0.006944 for the parameter $h_o t/k$. Subsequently, a change in the external resistances simulating boundary conditions at the heated surface resulted in a value of 0.02778 for this parameter. Figure 2 shows the results obtained from four identical configurations before and after this change was made. At the maximum passage spacing of twice the grid width, or 40 grid spaces, the data lie within a 6 percent band or within 3 percent of a mean line; at half that spacing agreement is better. On the basis of this agreement and the accuracy requirements of this project, it is felt that the use of a varying scale factor l in equation (2) to calculate R_{th}' for more than one geometrical configuration is justified within the range of $h_o t/k$ used herein.

Presentation of Results

Consider the heat-conduction equation

$$Q = \frac{kA}{l} \Delta T$$

or

$$\frac{l}{kA} = \frac{\Delta T}{Q}$$

[redacted]

The factor relating Q to ΔT is l/kA, which might be thought of as the resistance of the blade section to the flow of heat. The effects of cooling-passage geometry on this factor are investigated in this report. Obviously, k is independent of geometry, so that l/A and its variations with geometry are of principal concern. Inasmuch as the quantity involving Q', the heat flow per unit surface area, and ΔT will be of direct interest to the users of these data, $k\Delta T/Q'$ will be used in the figures presenting results rather than the identical quantity l/A; Q' is used rather than Q so that all results will be based on a common surface area and be directly comparable.

Application to Turbine-Cooling Calculations

In a typical application of the information herein, the designer will have to select a turbine blade-cooling configuration and a cooling system to operate within the limits imposed by engine and flight conditions. This report furnishes temperature drops through the blade for a wide range of configurations so that the effect of such drops on thermal stresses within the blade, temperature levels within the blade, and temperature level and operation of the cooling system may be evaluated.

The designer must determine Q' (or ΔT) from the conditions of operation, select the passage configuration which most nearly matches that which he is considering, and, from the proper curves, determine the applicable value of $k\Delta T/Q'$. The temperature drop (or Q') is then determined from

$$\Delta T = \frac{k\Delta T}{Q'} \frac{Q'}{k}$$

After evaluating the relative effect of numerous configurations upon blade stresses and cooling-system operation, other considerations such as fabrication problems must be weighed before a final configuration is chosen.

The application of the data must be limited to such sections as can be approximated by square or rectangular portions of the blade that fulfill the boundary conditions. Figure 1(a) indicates several such blade sections.

RESULTS AND DISCUSSION

In order to determine quantitatively the relations between heat flow and various temperature drops within the metal of cooled turbine blades for a variety of cooling-passage sizes, shapes, and spacings, with varying wall thicknesses, the resistance to the flow of heat was evaluated for a large number of cooling configurations. Plots relating $k\Delta T/Q'$ to

the geometry of the cooling-passage configurations are presented in terms of the average, the minimum, and the maximum heated-surface-to-cooled-surface temperature drop and the maximum temperature drop from the rear boundary of the blade section to the cooled surface. Initially, the depth of the simulated blade section was kept sufficiently large with respect to passage dimensions to approximate the condition of infinite section depth. Subsequently, the depth of section was gradually reduced and a number of cooling configurations were reinvestigated in order that the effect of section depth might be evaluated.

Resistance to Heat Flow Based on Average Heated-Surface Temperature

Maximum section depth. - Square passages: Typical results obtained with square passages in a section whose depth is large with respect to passage dimensions are shown in figure 3. Data are given for square passages of varying sizes at spacings of 0.8 and 0.2 inch. The curves showing the variation $k\overline{\Delta T}/Q'$ with wall thickness are parallel to that calculated for a plane wall except at low wall thicknesses. The curve for a plane wall which is heated uniformly on one side and cooled uniformly on the other represents the lower limit for such a series of curves; in this condition heat flows at a uniform density by the shortest possible path from the heated to the cooled surface. Any deviations from this condition require longer heat-flow paths and local increases in heat-flux densities, both of which increase the over-all resistance to heat flow. It is possible to have a much larger cooled surface area than occurs with a plane wall and still have a higher resistance to the flow of heat. With the 0.2-inch spacing (fig. 3(b)), any passage less than 0.2 but greater than 0.05 inch square will present more passage surface area to the heat flow than does the plane wall for the corresponding width of section, but the factors mentioned result in higher resistances to heat flow.

In comparing these and subsequent figures in which spacings vary, it must be remembered that all data are presented on the basis of a common heated-surface area. At comparable heat-flux densities at the heated surface, the smaller number of passages of a given size which are associated with the larger spacings require longer heat-flow paths and greater local heat-flux densities in the neighborhood of the cooling passages, with an accompanying increase in the over-all thermal resistance of the configuration.

If thermal resistances were calculated on the basis of the temperature differences between the cooling passage and the heated surface at a point directly opposite the passage, thermal resistances would go to zero at zero wall thickness. However, as the differences between cooling-passage temperatures and the average heated-surface temperatures were

used, finite values were obtained at zero wall thickness. The increases in flow resistance with decreasing wall thickness that are evident at very small wall thicknesses may be attributed to the influence of the steep temperature gradients in the immediate neighborhood of passages upon the outer surface temperatures.

The fact that the curves of $k\overline{\Delta T}/Q'$ against wall thickness are parallel to that for a plane wall (see fig. 2) makes possible the elimination of wall thickness as a variable if the deviations from a straight line at very small wall thicknesses may be ignored. The difference between $k\overline{\Delta T}/Q'$ for a given configuration and for a plane wall may be plotted against passage size with spacing as a parameter. In such a plot the curves of figure 3 appear as points, and a series of curves as shown in figure 3(a) appears as a single curve. This type of plot for a series of square-passage sizes and spacings is presented in figure 4(a). As passage sizes approach zero, heat-flow areas at the passage surfaces become very small and temperature gradients increase rapidly; the curves of figure 4(a) therefore go to infinity at zero passage size. As passages increase in size, flow conditions approach those through a plane wall. When the hole size equals the spacing for square holes, the plane-wall condition is reached and the curves go to zero.

Circular passages: Circular passages were investigated over a range of hole sizes, spacings, and wall thicknesses; results are presented in figure 4(b). Since the perimeter of the circular passage is smaller than that of a square whose sides equal the circle diameter, local heat-flux densities adjacent to the circular passage are higher, temperature gradients are steeper, and the resistance to heat flow is greater (cf. figs. 4(a) and (b)). As diameters increase, overlapping circular passages approach the plane-wall case only in the limit; the curves of figure 4(b) therefore approach the abscissa asymptotically rather than going to zero when passage diameters equal passage spacing.

Rectangular passages: The effect of using coolant passages of varying width-depth ratios is shown in figure 5, which indicates that passage width has much more effect upon the thermal resistance of the blade section than does the passage depth (cf. curve slopes, figs. 5(a) and (b)). Because of the relatively minor effect of passage depth, the curves of figure 5(b), which illustrate the effect of passage width, are limited to a single passage depth rather than covering a range of depths. The passage sizes shown are in the range of current interest in turbine cooling. Although the data apply directly to rectangular passages, they should permit estimation of $k\overline{\Delta T}/Q'$ for oval passages with reasonable accuracy.

Varying section depths (square passages). - The foregoing results were obtained with a constant section depth that was large with respect to passage dimensions. Figure 6 summarizes comparable results for several passage sizes when the section depth is reduced by steps to a

fraction of its original value. At small spacings and the larger passage sizes, the reduced section depth has little effect on $k\overline{\Delta T}/Q'$. As spacings increase and passage sizes decrease, pronounced increases in $k\overline{\Delta T}/Q'$ are evident.

For a given hole size and spacing, a separate curve of $k\overline{\Delta T}/Q'$ against wall thickness may be obtained for each section depth. As is evident from figure 6, the lower limit is that curve which applies for an infinite section depth, a condition which was approximated in the previous cases where section depth was large with respect to passage dimensions (figs. 3 to 5). The second limit for each family of curves is indicated by the dashed lines in figure 6, which apply to coolant passages at the extreme rear of the various sections. The sharp increase in $k\overline{\Delta T}/Q'$ that occurs as the rear boundary of the section is approached results from the reduction in flow area and the accompanying increase in thermal gradients in the region adjacent to the cooling passage. As spacings are reduced and passage sizes increased, these limiting curves approach each other and, for practical purposes, coincide.

Section heated along two opposing sides. - The case of a section of blade heated uniformly along two opposing sides and cooled by a single row of passages equidistant from those surfaces is illustrated in figure 7. Square and rectangular passages are considered. Inasmuch as Q' is defined as heat flux per unit surface area, it is obvious that the thermal resistance of a given section heated along one surface is the same as that of two such sections back to back. Therefore, the dashed curves of figure 6, which represent $k\overline{\Delta T}/Q'$ of sections heated along one surface and cooled by passages at the extreme rear, must also represent $k\overline{\Delta T}/Q'$ of sections heated along opposing surfaces and cooled at the centerline by a row of passages of the same width but twice the depth of the original passages. Figure 7 was evaluated in this manner from data such as those presented in figure 6.

Resistance to Heat Flow Based on Minimum Heated-Surface Temperature

The temperature gradients are greater along a normal from the heated surface to the center of the coolant passage than along any other heat-flow path in the section. The local heated-surface temperature is a minimum on this normal. The data in this section are based on the difference between this minimum heated-surface temperature and the cooled-surface temperature. The method of presentation is the same as in the preceding section.

Maximum section depth. - Square passages: The variations of $k\Delta T_{min}/Q'$ with wall thickness for the case of square passages in relatively deep sections are shown in figures 8(a) and (b) for passage

[redacted]

spacings of 0.4 and 0.2 inch, respectively. The magnitudes of the ordinates are, of course, lower for comparable conditions than those of curves based on the average heated-surface temperatures (see fig. 3). The rates at which curves become parallel to that for the plane wall is slower than was the case for curves based on average heated-surface temperatures (see fig. 3). This fact makes impractical the elimination of wall thickness as a variable. Consequently, data are presented in plots of $k\Delta T_{min}/Q'$ against wall thickness for a series of individual passage sizes rather than in plots of $(k\Delta T_{min}/Q') - (k\Delta T/Q')_{pw}$ against passage dimensions.

Circular passages: Figures 8(c) and (d) show the variation of $k\Delta T_{min}/Q'$ with wall thickness for circular passages in a relatively deep section for passage spacings of 0.4 and 0.2 inch. Values of $k\Delta T_{min}/Q'$ for circular passages are slightly higher at comparable conditions than for square passages whose sides are equal to the diameter of the circular passages. Again, it is evident that magnitudes of $k\Delta T_{min}/Q'$ are lower at comparable conditions than for curves based on average heated-surface temperatures.

Varying section depths (square passages). - The variation of $k\Delta T_{min}/Q'$ with wall thickness for a series of section depths is shown in figure 9 for a range of square-passage sizes and spacings. The comparison made previously for similar data based on average heated-surface temperatures is applicable in the present case, both as to magnitude of ordinates and rates at which the slopes of curves approach that of the plane wall.

Section heated along two opposing sides. - The variation of $k\Delta T_{min}/Q'$ with wall thickness is shown in figure 10 for a section heated along two opposing sides and cooled by a single row of passages along its centerline. Curves vary from those based on $\overline{\Delta T}$ (fig. 7), in that they go to zero when section thickness equals passage depth, and their slopes approach that of a plane wall at a slower rate.

Resistance to Heat Flow Based on Maximum Heated-Surface Temperature

In order to permit calculations for the maximum temperature, figures 11 to 13 have been prepared. The data differ from those previously shown only in the temperature drop involved, the drop from the heated surface at a point equidistant from the passages to the cooled surfaces.

Maximum section depth. - Square passages: The variation of $k\Delta T_{max}/Q'$ with wall thickness is shown in figure 11(a) for square passages in a relatively deep section. The curves are, in general, similar to those based on average surface temperatures (fig. 3). Aside from magnitudes, the chief difference lies in the rate at which the curves become parallel to that for the plane wall. In the present instance, the rate is much slower than noted previously, particularly at the larger passage spacings.

Circular passages: The variation of $k\Delta T_{max}/Q'$ with wall thickness is given in figure 11(b) for circular passages in a relatively deep section. The remarks concerning square passages apply equally here. As noted previously, magnitudes of $k\Delta T_{max}/Q'$ are higher for circular passages of a given diameter than for the comparable square passages.

3883

Varying section depths (square passages). - The maximum temperatures that occur on the heated surfaces of sections of varying depths may be determined for a number of passage sizes from the data of figure 12. In general, the curves are quite similar to those based on average and minimum surface temperatures. Magnitudes of $k\Delta T_{max}/Q'$ are, of course, greater. The rates at which the curves become parallel to that for the plane wall are slower than those of $k\overline{\Delta T}/Q'$ in this case also.

Section heated along two opposing sides. - The maximum temperatures on the blade surface may be determined from figure 13 for a section heated along opposing sides and cooled by a single row of passages along the centerline. Magnitudes are greater than in figure 7 where average heated-surface temperatures were used rather than maximum values, and figure 10 where minimum heated-surface temperatures were used. Slopes of the corresponding curves vary appreciably, but the plots are basically the same.

Resistance to Heat Flow Based on Maximum Rear-Boundary Temperature

In order to give a rough idea of temperature variations in the region behind the cooling passages with various cooling-passage configurations, a series of curves is shown which is based on the differences between the maximum temperature on the section boundary opposite the heated surface and the temperature at the cooling-passage surface (figs. 14 and 15). The maximum rear-boundary temperature corresponds to the maximum temperature at the centerline of a turbine blade. If Q', k, and the cooled-surface temperature are known, the maximum rear-boundary temperature may be evaluated from these figures.

Varying section depths (square passages). - The variations of $k\Delta T_r/Q'$ with wall thickness are shown for three square-passage sizes in figure 14 for a range of section depths and passage spacings. As might be expected, the magnitude of $k\Delta T_r/Q'$ is very sensitive to passage size and passage spacing. The limiting condition here, which corresponds to the plane-wall case shown in many of the preceding figures, is the horizontal coordinate axis; this condition corresponds to the complete isolation of the core of the blade by the coolant. Some of the configurations illustrated in figure 14 approach this limiting condition closely.

Section heated along two opposing sides (square passages). - As in previous cases, the dashed curves of figure 14, for passages at the extreme rear of the simulated blade section, are extended in figure 15 to represent conditions for sections heated uniformly along two opposing sides. At low wall thicknesses or low section thicknesses, the temperature midway between cooling passages is sensitive to wall thickness; but, as wall thicknesses increase, the curves flatten out and the temperature at that point remains almost constant.

ILLUSTRATIVE EXAMPLE

The following example is included to indicate the magnitudes of the temperature drops within a turbine blade with various passage geometries.

Assume that a portion of a blade may be approximated by a 1- by 1- by 0.15-inch section. Operating conditions yield an effective gas temperature of 1600° F and a surface heat-transfer coefficient of 225 Btu/(hr)(sq ft)(°F). Stress considerations indicate that an average metal temperature on the order of 1300° F will be permissible; at this temperature the blade material has a thermal conductivity of 14 Btu/(hr)(ft)(°F). Evaluating Q' from surface conditions gives

$$Q' = h(T_{g,e} - \overline{T}_o) = 225 \times \frac{1}{144} \times (1600 - 1300) = 469 \text{ Btu/(hr)(sq in.)}$$

$$\frac{Q'}{k} = \frac{469}{14 \times \frac{1}{12}} = 402^\circ \text{ F/in.}$$

For a 1- by 1- by 0.15-inch section with a 0.05-inch wall, a 0.2-inch passage spacing, and a passage size of 0.04 by 0.04 inch, figure 6(b) gives a value of 0.085 for $k\overline{\Delta T}/Q'$. Then,

$$\overline{\Delta T} = \frac{k\overline{\Delta T}}{Q'} \times \frac{Q'}{k} = 0.085 \times 402 = 34.2^\circ \text{ F}$$

[redacted]

For the same conditions, figure 9(b) yields a value for $k\Delta T_{min}/Q'$ of 0.071, from which $\Delta T_{min} = 0.071 \times 402 = 28.5^{\circ}$ F. Similarly, from figure 12(b), $k\Delta T_{max}/Q' = 0.085$ and $\Delta T_{max} = 34.2^{\circ}$ F. At the rear of the section (fig. 14(b)), $k\Delta T_r/Q' = 0.023$ and $\Delta T_r = 9.2^{\circ}$ F.

For comparison, table II summarizes the temperature differences obtained at four passage spacings for (a) a 0.04- by 0.04-inch passage with a section depth of 0.15 inch, (b) a 0.04- by 0.04-inch passage with a very large section depth, and (c) a 0.04-inch-diameter passage with a very large section depth.

Under the conditions chosen, the temperature drops are very similar; variations due to section depth or to differences in flow paths for square and circular passages are slight at spacings of 0.4 inch or less. With smaller section depths, smaller passages, and larger passage spacings, the variations would, of course, be more pronounced.

In designing a blade for maximum blade and coolant temperatures, a series of such calculations may be made in order to survey a wide range of geometries and arrive at a tentative configuration or configurations. Then, if desired, a more accurate and detailed knowledge of blade temperature distribution may be obtained either by relaxation methods or by the use of analogs. In either case, a larger section of the blade profile should be examined than in the present investigation.

In the final selection of a configuration, thermal stresses due to temperature gradients, centrifugal stresses arising from the load due to the weight of the coolant within the blade, and pressure forces resulting from centrifugal action on the coolant must be weighed in relation to the over-all mechanical design of the blade.

CONCLUDING REMARKS

Experimentally determined curves are presented which show quantitatively the effect of cooling-passage geometries upon the relations between heat flow and temperature drops within cross sections of liquid-cooled turbine blades. Temperature differences between the cooled surfaces and points of (1) average, (2) minimum, and (3) maximum heated-surface temperatures and (4) maximum centerline temperatures may be evaluated for a wide range of cooling-passage sizes, shapes, spacings, and wall thicknesses and for a range of blade-section thicknesses. Such information will be required in designing liquid-cooled blades and liquid-filled cooling systems for maximum-temperature operation in aircraft turbines.

Lewis Flight Propulsion Laboratory
National Advisory Committee for Aeronautics
Cleveland, Ohio, November 25, 1955

[redacted]

APPENDIX - ANALOG PRINCIPLES AND DESIGN

Principles

The difficulties involved in obtaining accurate experimental thermal measurements are such that, for over a half a century, scientists have been developing ways of evaluating thermal relations from experimental measurements of quantities other than heat flow and temperature. The field of application is wide, since analytical methods, except in the simplest cases, are cumbersome and lengthy. Analogy methods have served well.

Equations. - This section is taken almost directly from the discussion of Jakob in reference 6 for steady-state conditions.

Consider a homogeneous body of thermal conductivity k which has a heated surface A_1 at a uniform temperature T_1 and a cooled surface A_2 at temperature T_2 and is thermally insulated elsewhere. Heat flow will be in accordance with Laplace's equation:

$$\frac{\partial^2 T}{\partial x^2} + \frac{\partial^2 T}{\partial y^2} + \frac{\partial^2 T}{\partial z^2} = 0 \tag{A1}$$

The heat-flow rate is given by

$$Q = - k \int_{A_1} \frac{\partial T}{\partial n} \, dA_1 \tag{A2}$$

where n is the direction normal to dA_1.

Let

$$\Phi = \frac{T - T_2}{T_1 - T_2} \tag{A3}$$

Substitution of equation (A3) in equation (A1) yields

$$\frac{\partial^2 \Phi}{\partial x^2} + \frac{\partial^2 \Phi}{\partial y^2} + \frac{\partial^2 \Phi}{\partial z^2} = 0 \tag{A4}$$

with the boundary conditions

$$\Phi = 1 \quad \text{for} \quad T = T_1$$

$$\Phi = 0 \quad \text{for} \quad T = T_2$$

[redacted]

Equation (A2) becomes

$$Q = k(T_1 - T_2) \int_{A_1} - \frac{\partial \Phi}{\partial n} dA_1 \qquad (A5)$$

Hence, neither Φ nor the integral of equation (A5) depends on temperatures but only upon the shape of the body.

The integral of equation (A5) may be considered as the ratio of the mean effective area of the heat-flow path to the mean effective length. Since this ratio is independent of both temperature and heat flow, it can be determined by any suitable experimental method that satisfies equations (A1) and (A2), regardless of the quantities represented by T, Q, and k, as long as the experimental shape is similar to the body under consideration.

Electrical analogy. - In employing an electrical system to simulate heat flow through a body, the analogy between the various quantities becomes apparent from examination of the equations involved. Consider the electrical conduction equation

$$\Delta e = iR_E \qquad (A6)$$

and the thermal conduction equation

$$\Delta T = Q \frac{l}{kA} \qquad (A7)$$

The driving force is Δe in one case and ΔT in the other, the current flow i corresponds to the heat-flow rate Q, and the electrical resistance R_E has its counterpart in the thermal flow resistance l/kA.

In geometrically similar flow paths, definite relations exist between these corresponding quantities. The temperature gradients and heat-flow rates in each local area of the heat-flow system bear the same relations to the potential gradients and current flow rates in the corresponding area of the electrical model as the over-all temperature drop and the total heat flow of the heat-flow system do to the total voltage drop and the total current flow through the electrical model.

Design

General considerations. - A number of mediums have been employed to simulate bodies in which heat-flow relations were being considered. Availability of equipment and materials and ease of handling plus some

previous experience in fabrication led to the selection of a simple resistance-wire grid (see fig. 1(c)) for the present project. As long as a relatively large number of mesh are used, the network of discrete lumped resistances approximates the condition of a continuous heat-flow path with sufficient accuracy for the problem. Accuracy within 1 to 5 percent may be attained with analogs of this type.

Design relations. - The relation between the thermal resistance of the body considered and the electrical resistance of the analog model depends on the electrical resistance of one side of a unit grid mesh on the analog and the thermal resistance of the metal block represented by that electrical resistance, or, in other words, on the scale of the model. Consider an analog in which the unit grid resistance R_w represents the thermal resistance R_{th} of a metal block of cross section $l \times L$ and of thickness t. The resistance of the block to the flow of heat is given by

$$R_{th} = \frac{t}{klL} \tag{A8}$$

Then,

$$\frac{R_{th}}{R_E} = \frac{t}{R_w k l L} \tag{A9}$$

This ratio governs the conversion of any resistance values obtained from the analog into the corresponding thermal resistances. It also controls the values of the electrical resistances required to represent the thermal resistances of the boundary layer at the outer surface of the simulated portion of the turbine blade. The resistance required for each surface area $l \times L$ is computed as follows:

$$R_{th,o} = \frac{T_{g,e} - \overline{T}_o}{Q} = \frac{1}{h_o A_o} = \frac{1}{h_o l L} \tag{A10}$$

$$R_{E,o} = R_{th,o} \frac{R_E}{R_{th}} = \frac{1}{h_o L l} \times \frac{R_w k l L}{t} = \frac{R_w k}{h_o t} \tag{A11}$$

Similar calculations may be made for the cooled surfaces if a finite heat-transfer coefficient is assumed there. In the present case, an infinite coefficient was assumed.

Analog design. - A 20- by 20-inch grid of 24-gage bright-drawn chromel wire was fabricated using a 1- by 1-inch grid mesh. The wire was calibrated and found to have a resistance of 0.0884 ohm per inch at 70° F.

[redacted]

The metal block represented on the grid by a 1-inch length of wire was assumed to have the dimensions L = 1 inch (perpendicular to the plane of the grid), l = 0.005 inch, and t = 0.005 inch. Values of h_o = 250 Btu/(hr)(sq ft)(°F) [1.736 Btu/(hr)(sq in.)(°F)] and k = 15 Btu/(hr)(ft)(°F) [1.25 Btu/(hr)(in.)(°F)] were chosen as typical of those encountered in cooled-turbine work. The temperature drop through the boundary layer at the cooled surfaces was assumed negligible in the present case in view of the strong cooling that may be realized with liquids. These values, when substituted in equations (A10) and (A11), yield the following:

$$\frac{R_{th}}{R_E} = 9.05 \text{ (hr)(°F)/(Btu)(ohm)}$$

$$R_{E,o} = 12.73 \text{ ohms}$$

A calibrated 28-gage chromel wire (resistance = 0.213 ohm per in. at 70° F) was used for $R_{E,o}$, 59.7 inches being required for each unit grid surface area $l \times L$.

It can be seen from equation (A11) that $h_o t/k = R_w/R_{E,o}$. The typical values assumed give a value of 0.006944 for this parameter. Subsequently, $R_{E,o}$ was arbitrarily reduced by a factor of 4 and the parameter increased to 0.02778 in order that the effect of changes in external heat-transfer coefficient and/or scale might be observed.

REFERENCES

1. Schmidt, E.: The Possibilities of the Gas Turbine for Aircraft Engines. Reps. & Trans. No. 489, GDC 2504T, British M.O.S.

2. Freche, John C., and Diaguila, A. J.: Heat-Transfer and Operating Characteristics of Aluminum Forced-Convection and Stainless-Steel Natural-Convection Water-Cooled Single-Stage Turbines. NACA RM E50D03a, 1950.

3. Schramm, Wilson B., Nachtigall, Alfred J., and Arne, Vernon L.: Analytical Comparison of Turbine-Blade Cooling Systems Designed for a Turbojet Engine Operating at Supersonic Speed and High Altitude. I - Liquid-Cooling Systems. NACA RM E52J29, 1953.

4. Livingood, John N. B., and Brown, W. Byron: Analysis of Temperature Distribution in Liquid-Cooled Turbine Blades. NACA Rep. 1066, 1952. (Supersedes NACA TN 2321.)

[redacted]

5. Ellerbrock, Herman H., Jr., Schum, Eugene F., and Nachtigall, Alfred J.: Use of Electric Analogs for Calculation of Temperature Distribution of Cooled Turbine Blades. NACA TN 3060, 1953.

6. Jakob, Max: Heat Transfer. Vol. I. John Wiley & Sons, Inc., 1949, p. 400.

[redacted]

TABLE I. - RANGE OF COOLING-PASSAGE GEOMETRIES INVESTIGATED

Temperature on which data are based	Passage shape	Passage size, in.	Passage spacing, in.	Wall thickness, in.	Section depth, in.	Number of heated surfaces
Average heated-surface	Square	0 to 0.6	0 to 0.8	0 to ∞	∞	1
	Circular	0 to 0.6	0 to 0.8	0 to ∞	∞	1
	Rectangular	0.02 deep; 0 to 0.6 wide	0.2 to 0.8	0 to ∞	∞	1
	Rectangular	0.02,0.04,0.06 wide; 0.01 to 0.06 deep	0.1 to 0.4	0 to ∞	∞	1
	Square	0.02	0 to 0.4	0 to 0.22	0.05 to 0.20	1
		0.04	0 to 0.4	0 to 0.22	0.10 to 0.25	1
		0.08	0 to 0.8	0 to 0.22	0.10 to 0.40	1
		0.12	0 to 0.8	0 to 0.22	0.15 to 0.40	1
	Square	0.02 to 0.08	0.2 to 0.4	0 to 0.2	0.02 to 0.40	2
	Rectangular	0.02×0.04 0.04×0.08	0.02 to 0.44	0 to 0.2	0.02 to 0.40	2
Minimum heated-surface	Square	0.02 to 0.12	0.2,0.4	0 to 0.2	∞	1
	Circular	0.03 to 0.20	0.2,0.4	0 to 0.2	∞	1
	Square	0.02 to 0.12	0.1 to 0.8	0 to 0.2	0.05 to 0.25	1
	Square	0.02 to 0.12	0.2,0.4	0 to 0.2	0 to 0.4	2
	Rectangular	0.02×0.04 0.04×0.08	0.2,0.4	0 to 0.2	0 to 0.4	2
Maximum heated-surface	Square	0.01 to 0.12	0 to 0.8	0 to 0.18	∞	1
	Circular	0.02 to 0.10	0 to 0.8	0 to 0.18	∞	1
	Square	0.02 to 0.06	0 to 0.4	0 to 0.20	0.05 to 0.25	1
	Square	0.02	0.2,0.4	0 to 0.20	0.10 to 0.40	2
	Rectangular	0.02×0.04 0.04×0.08 0.06×0.12	0.2,0.4	0 to 0.2	0.10 to 0.40	2
Maximum rear-boundary	Square	0.02,0.04,0.08	0.2 to 0.4	0 to 0.2	0.05 to 0.35	1
	Square	0.01,0.02,0.04	0.2 to 0.4	0 to 0.2	0 to 0.40	2
	Rectangular	0.02×0.04 0.04×0.08 0.08×0.16	0.2 to 0.4	0 to 0.2	0 to 0.40	2

[redacted]

TABLE II. - TEMPERATURE DROPS THROUGH BLADE OF ILLUSTRATIVE EXAMPLE

[Wall thickness, 0.05 in.]

Section depth, in.	Passage size, in.	Passage spacing, in.	$\frac{k\overline{\Delta T}}{Q'} - \left(\frac{k\Delta T}{Q'}\right)_{pw}$, in.	$\left(\frac{k\Delta T}{Q'}\right)_{pw}$, in.	$\frac{k\overline{\Delta T}}{Q'}$, in.	$\overline{\Delta T}$, °F	$\frac{k\Delta T_{min}}{Q'}$, in.	ΔT_{min}, °F	$\frac{k\Delta T_{max}}{Q'}$, in.	ΔT_{max}, °F	$\frac{k\Delta T_r}{Q'}$, in.	ΔT_r, °F
0.15	0.04× 0.04	0.1			Fig. 6(b) 0.061	24.5	Fig. 9 ------	----	Fig. 12(b) 0.063(est)	25.2	Fig. 14(b) ----------	----
		.2			.085	34.2	0.071	28.5	.085	34.2	0.020	8.0
		.4			.162	64.8	.097	39.0	.195	78.4	.128	51.4
		.8			-----	----	-----	----	-----	----	-----	----
∞	0.04× 0.04	0.1	Fig. 4(a) 0.011	Fig. 3 0.050	0.061	24.9	Fig. 8 ------	----	Fig. 11(a) 0.06(est)	24.1		
		.2	.035	↓	.085	34.2	0.070	28.1	.075	30.3		
		.4	.092		.142	57.1	.096	38.6	.181	72.8		
		.8	.26(est)		.31	125	-----	----	.44	177		
∞	0.04 diam	0.1	Fig. 4(b) 0.0135	Fig. 3 0.050	0.0635	25.5	Fig. 8 ------	----	Fig. 11(b) 0.055(est)	22.0		
		.2	.034	↓	.084	33.3	0.073	29.3	.079	31.8		
		.4	.100		.150	60.3	.096	38.6	.185	74.4		
		.8	.27(est)		.32	128.5	-----	----	.500	201		

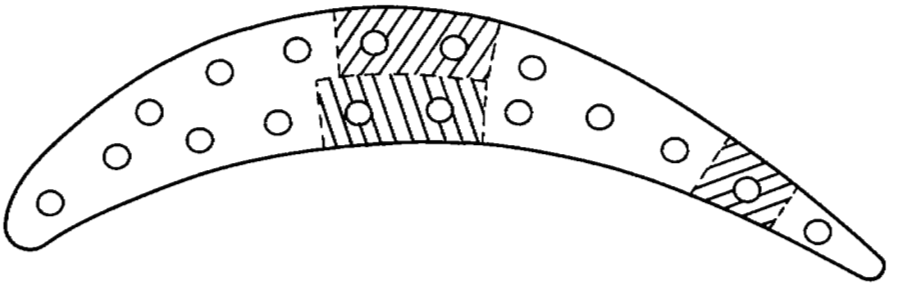

(a) Typical regions that may be approximated on rectangular analog.

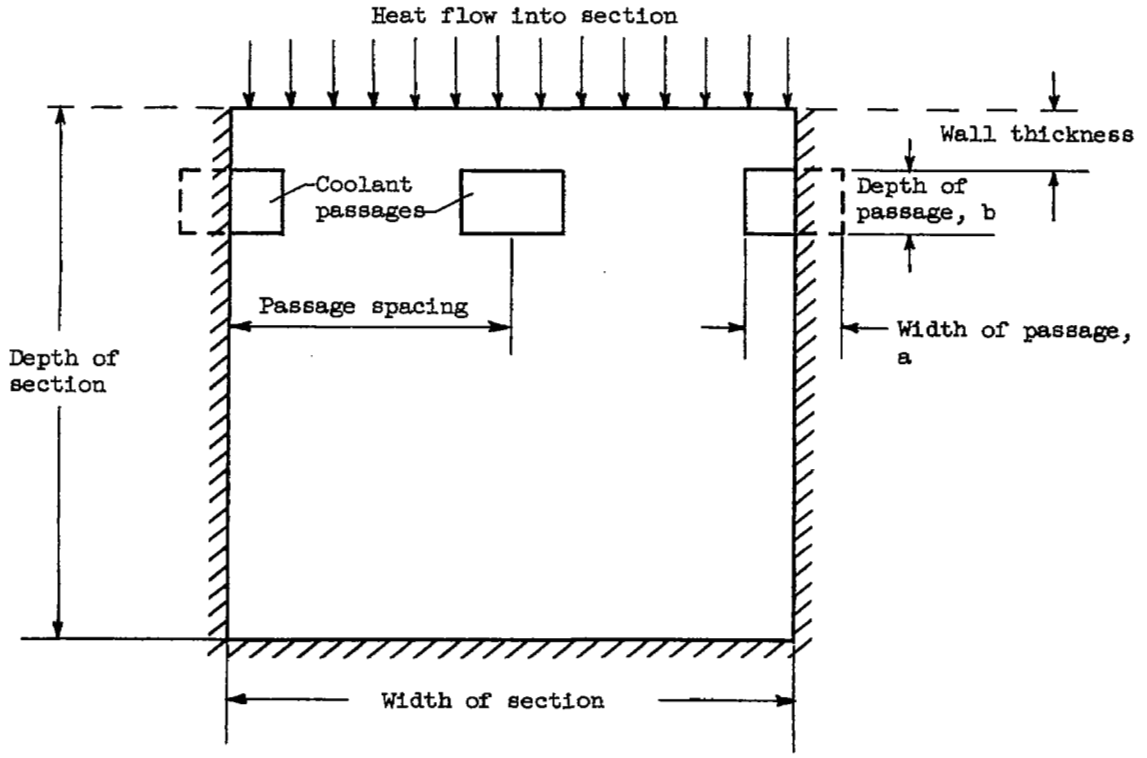

(b) Idealized blade section represented by experimental setup.

Figure 1. - Relations of cooled-turbine-blade sections to experimental analog.

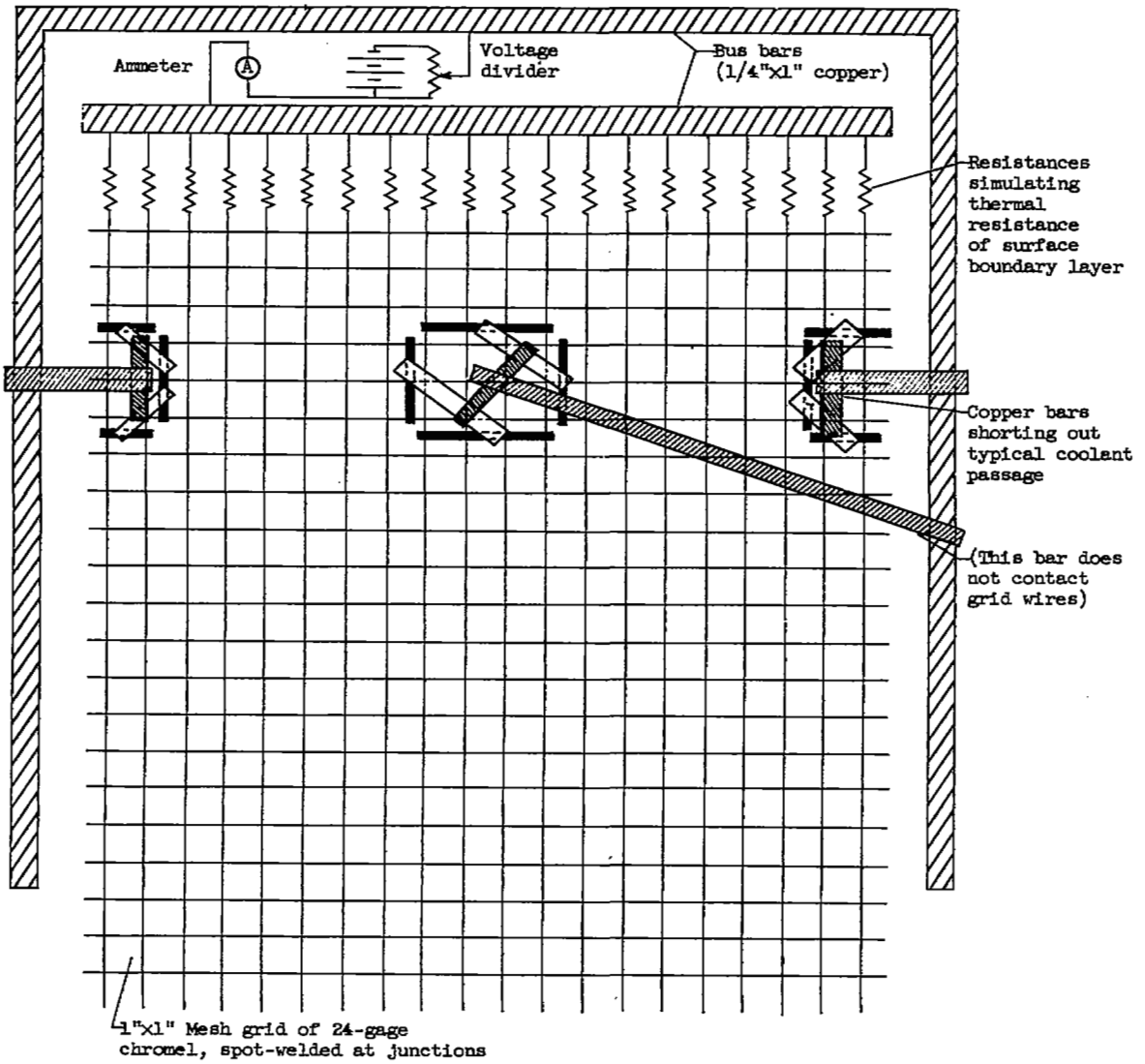

(c) Schematic drawing of experimental analog.

Figure 1. - Continued. Relations of cooled-turbine-blade sections to experimental analog.

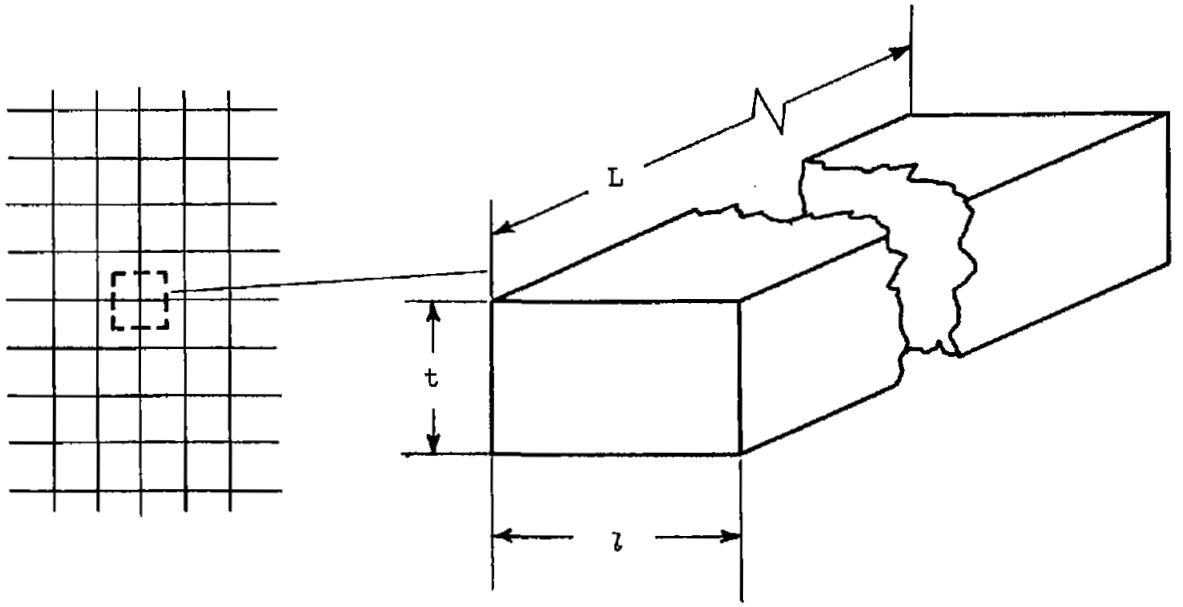

(d) Metal block whose thermal resistance is represented by 1- by 1-inch segment of grid.

Figure 1. - Concluded. Relations of cooled-turbine-blade sections to experimental analog.

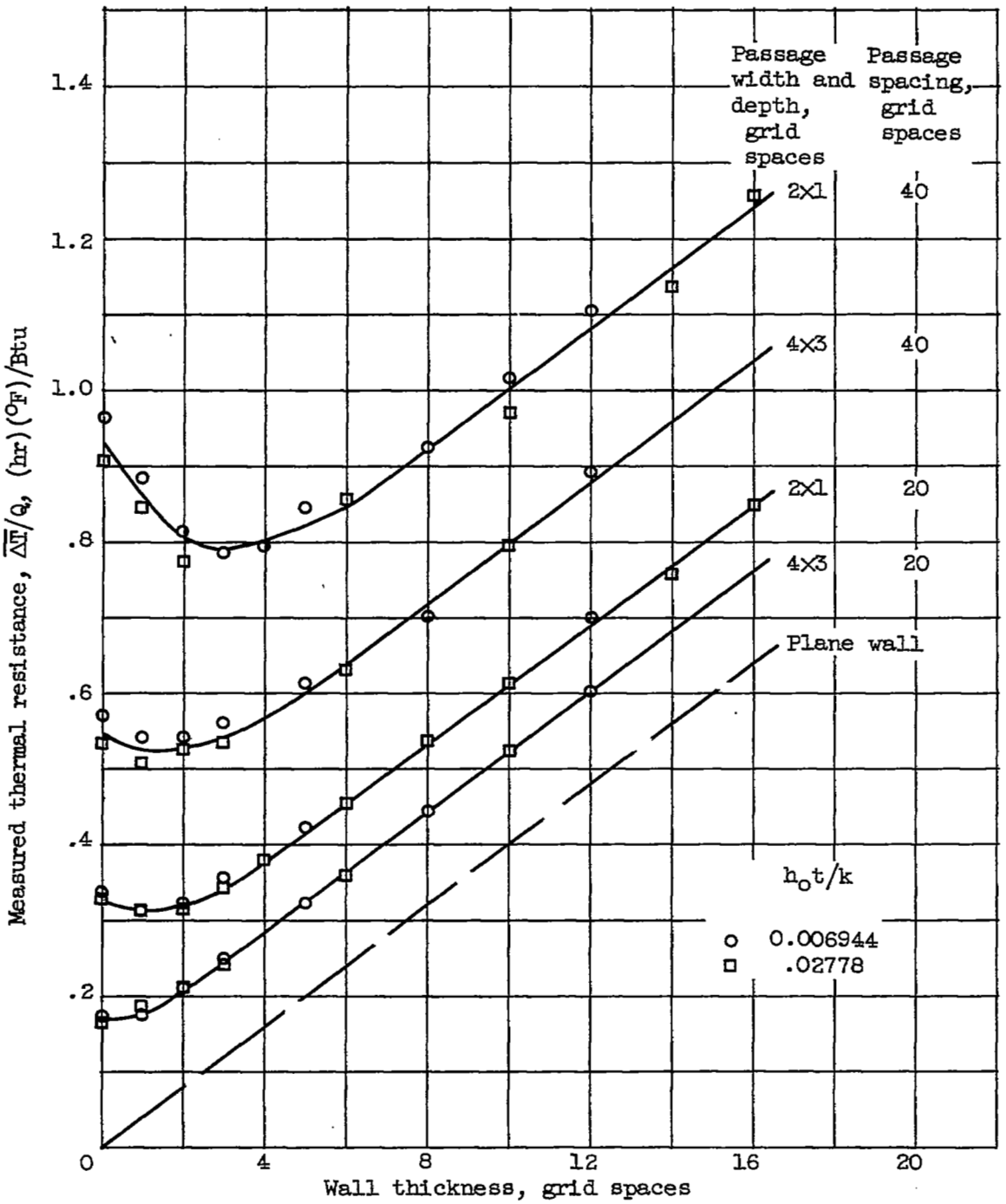

Figure 2. - Effect of fourfold variation of parameter $h_o t/k$ on measured thermal resistance.

[redacted]

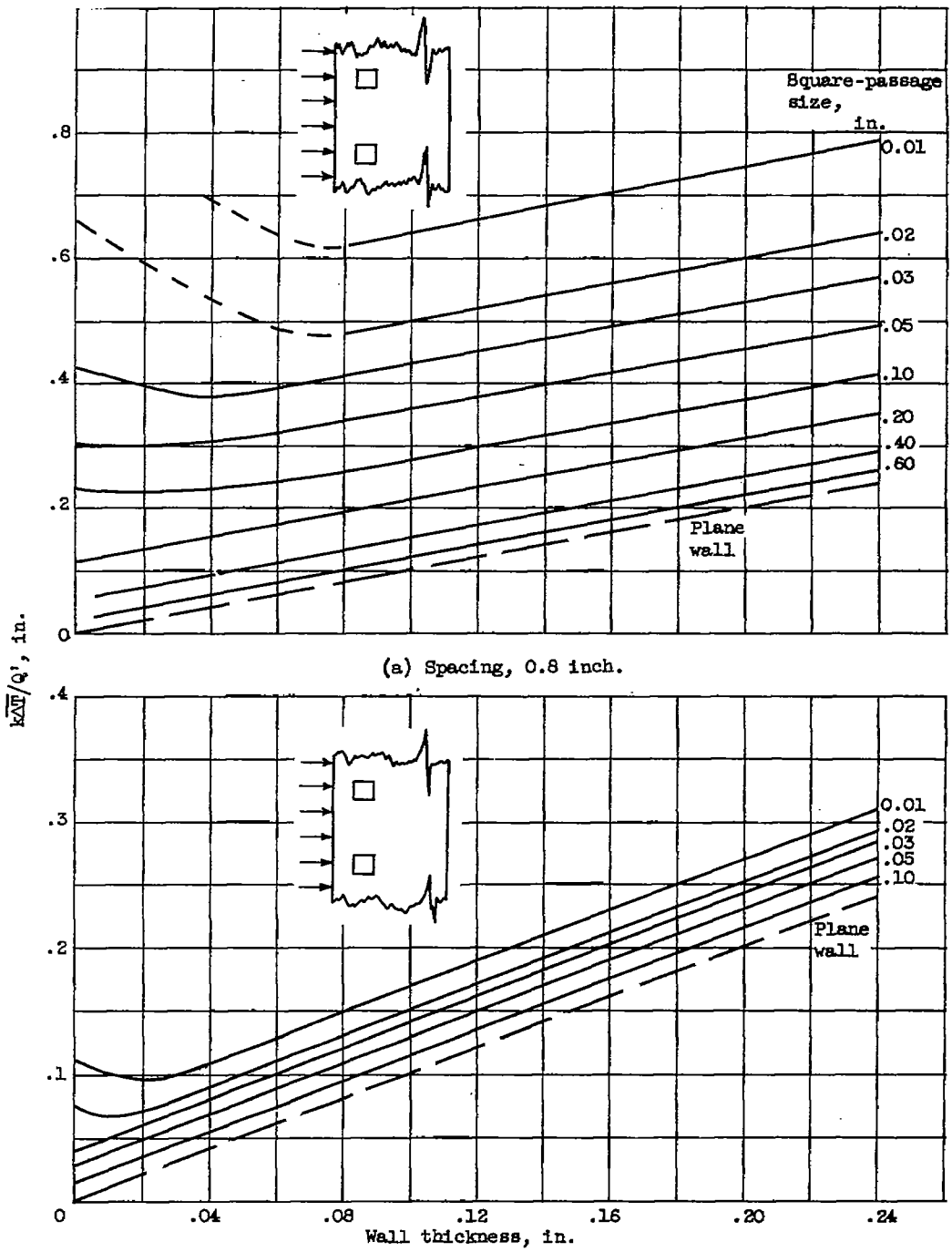

(a) Spacing, 0.8 inch.

(b) Spacing, 0.2 inch.

Figure 3. - Typical variation of $k\overline{\Delta T}/Q'$ with wall thickness in section whose depth is large with respect to passage dimensions. Square passages.

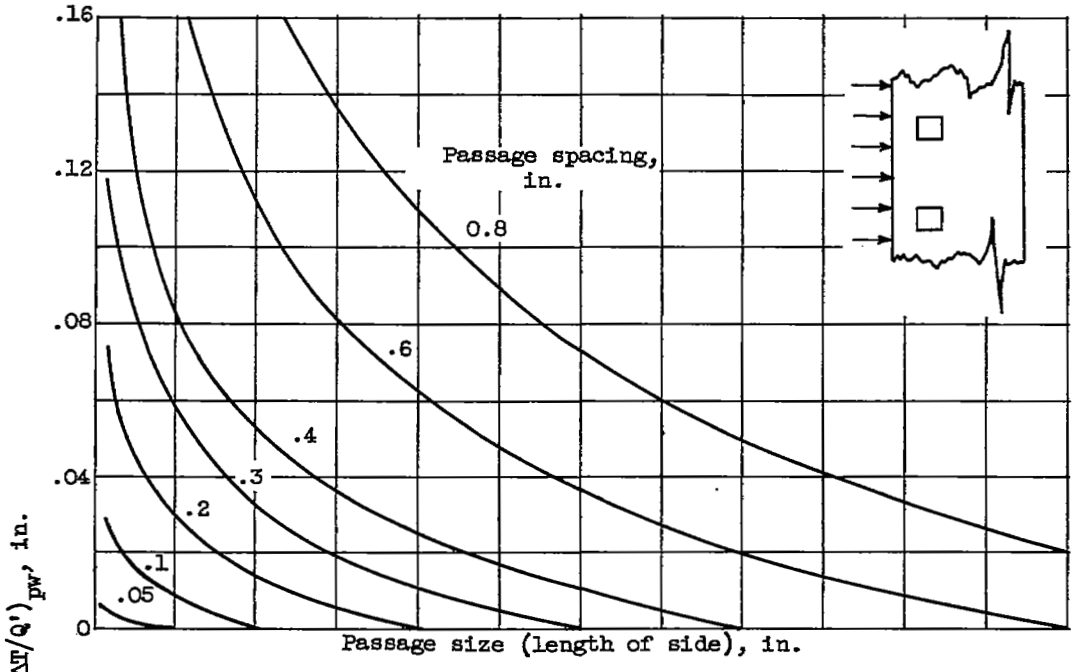

(a) Square passages.

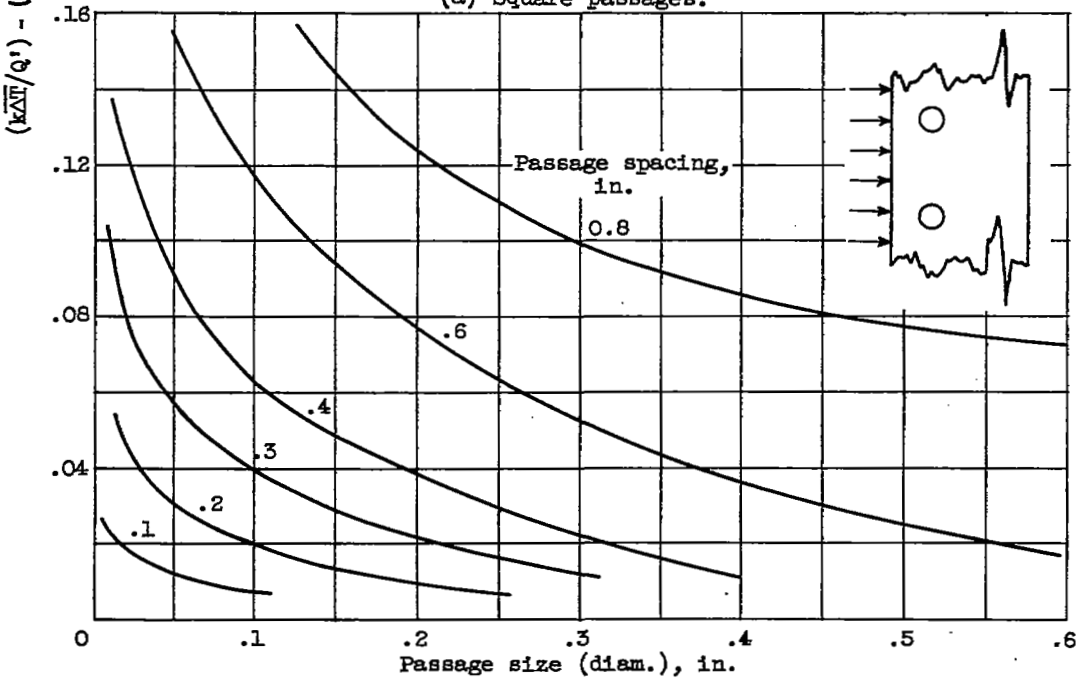

(b) Circular passages.

Figure 4. - Variation of $(k\Delta\overline{T}/Q') - (k\Delta T/Q')_{pw}$ with passage size in section whose depth is large with respect to passage dimensions.

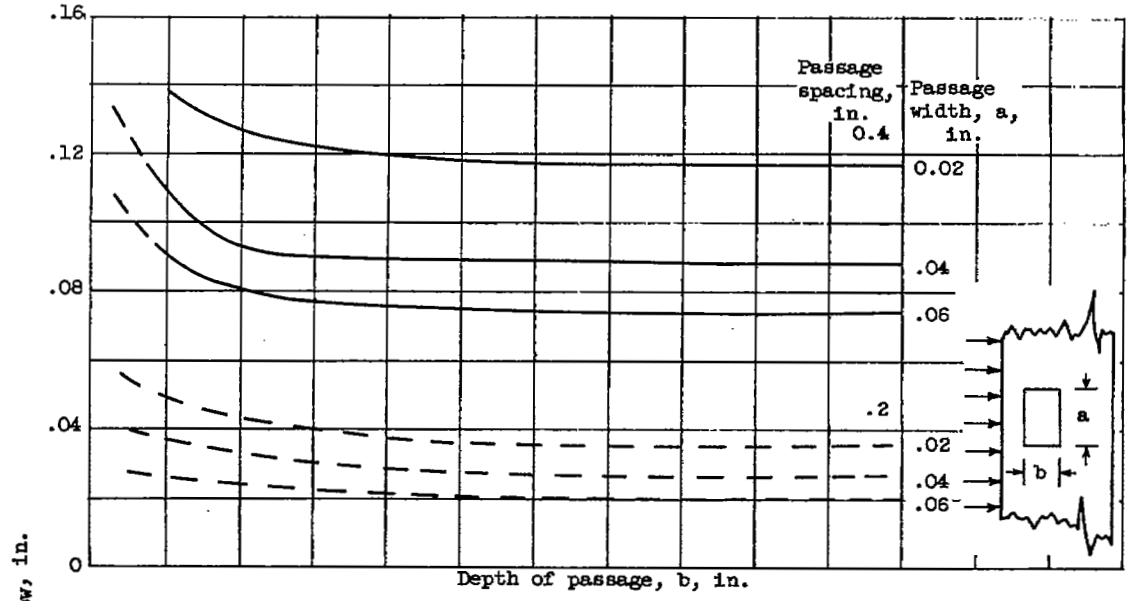

(a) Depth of passage variable; width, 0.02, 0.04, and 0.06 inch.

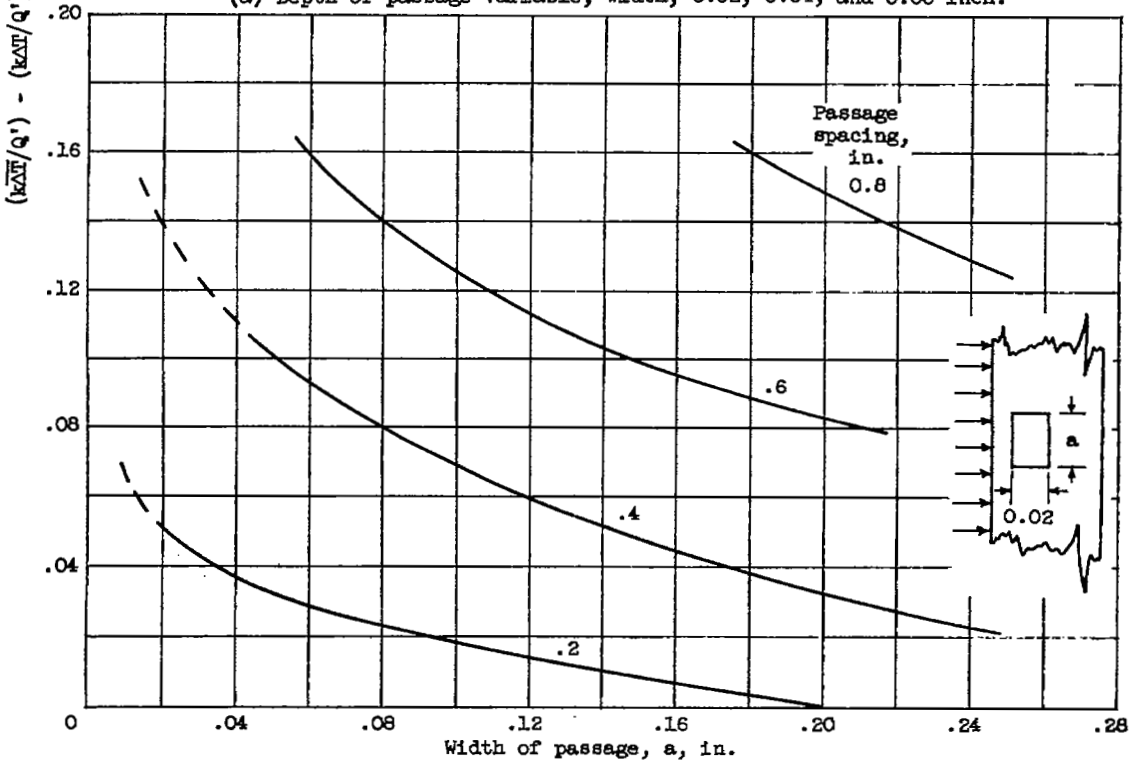

(b) Width of passage variable; depth, 0.02 inch.

Figure 5. - Variation of $(k\Delta\overline{T}/Q') - (k\Delta T/Q')_{pw}$ with passage size and spacing for various width-depth ratios in section whose depth is large with respect to passage dimensions.

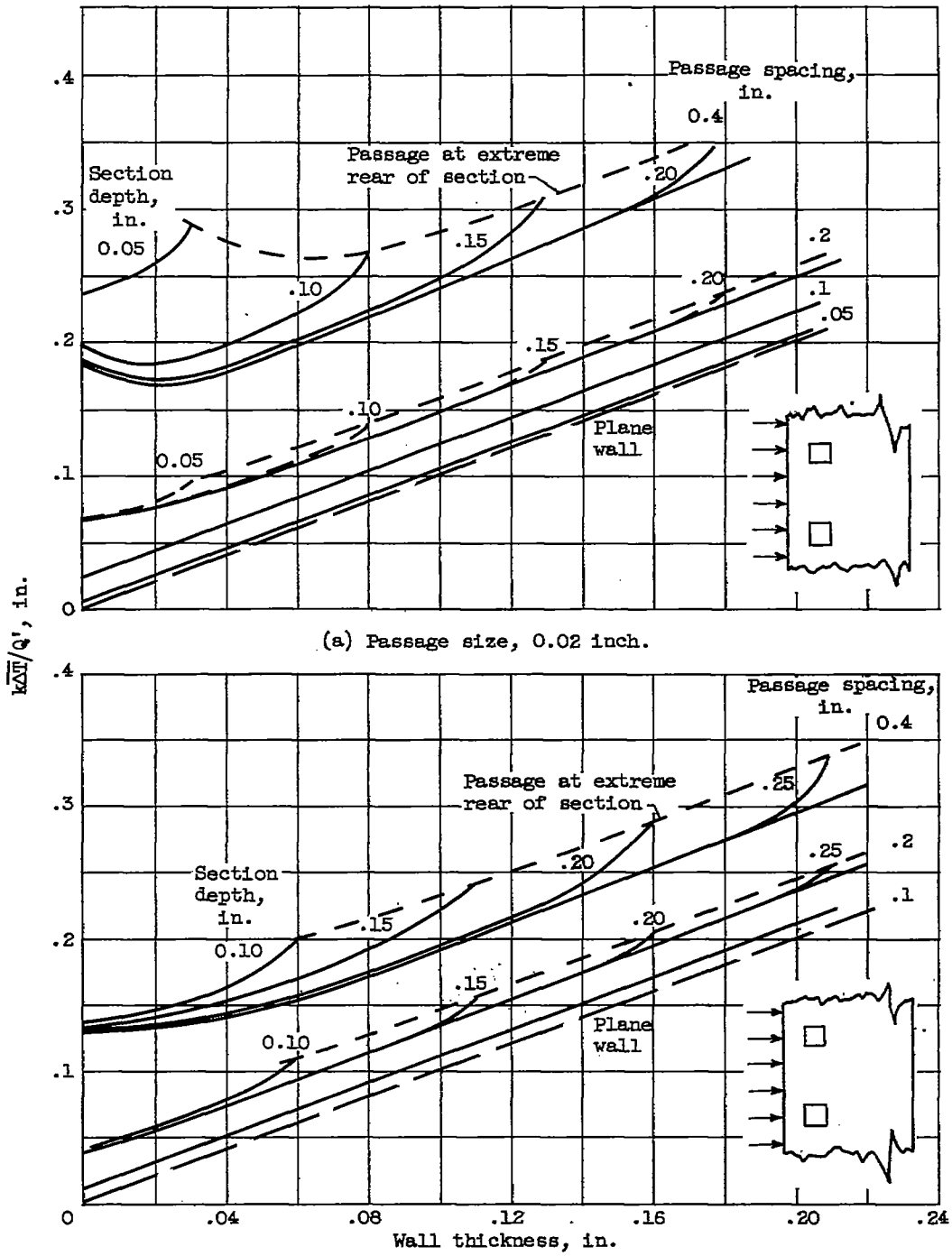

(a) Passage size, 0.02 inch.

(b) Passage size, 0.04 inch.

Figure 6. - Variation of $k\overline{\Delta T}/Q'$ with wall thickness at various section depths and passage spacings. Square passages.

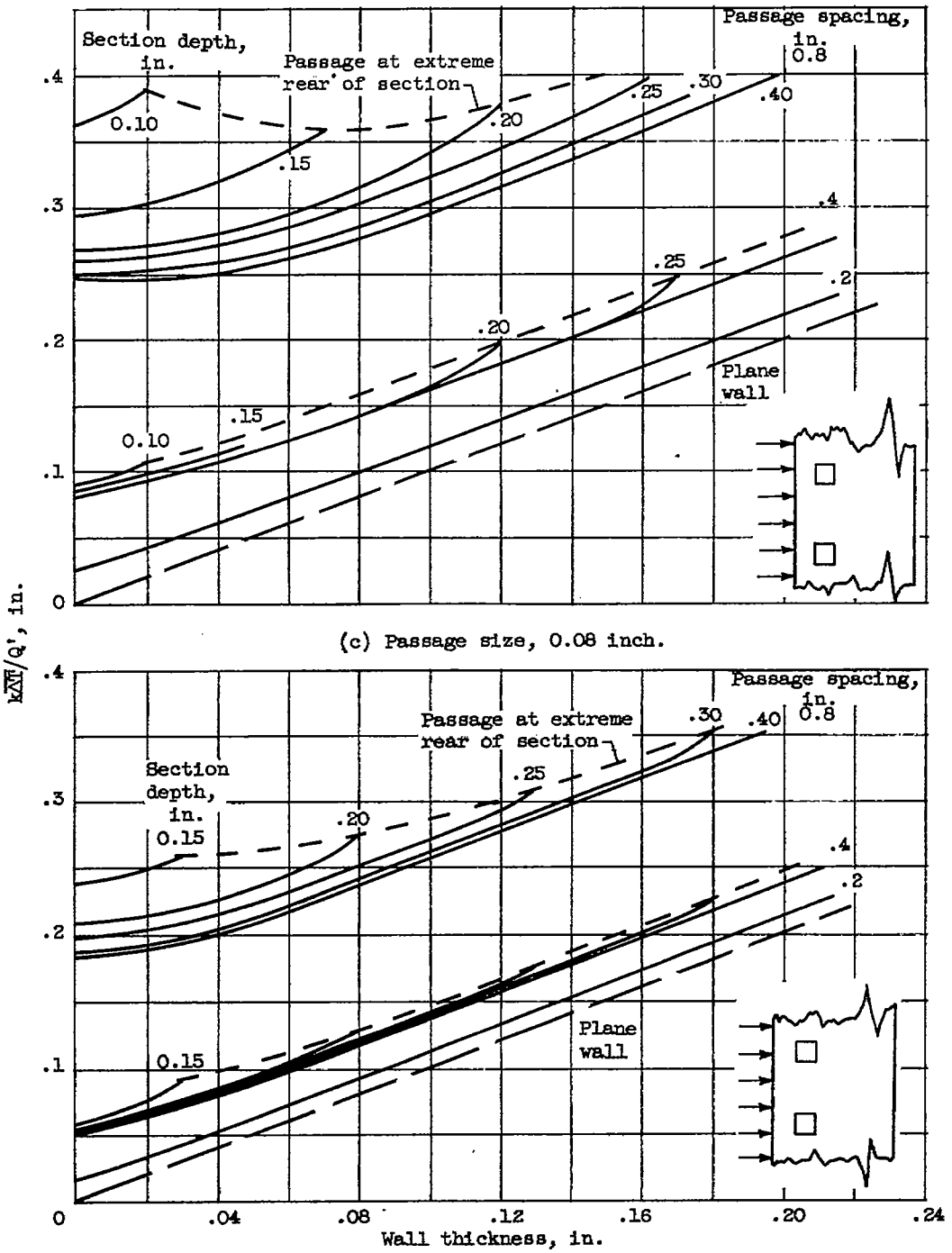

(c) Passage size, 0.08 inch.

(d) Passage size, 0.12 inch.

Figure 6. - Concluded. Variation of $k\overline{\Delta T}/Q'$ with wall thickness at various section depths and passage spacings. Square passages.

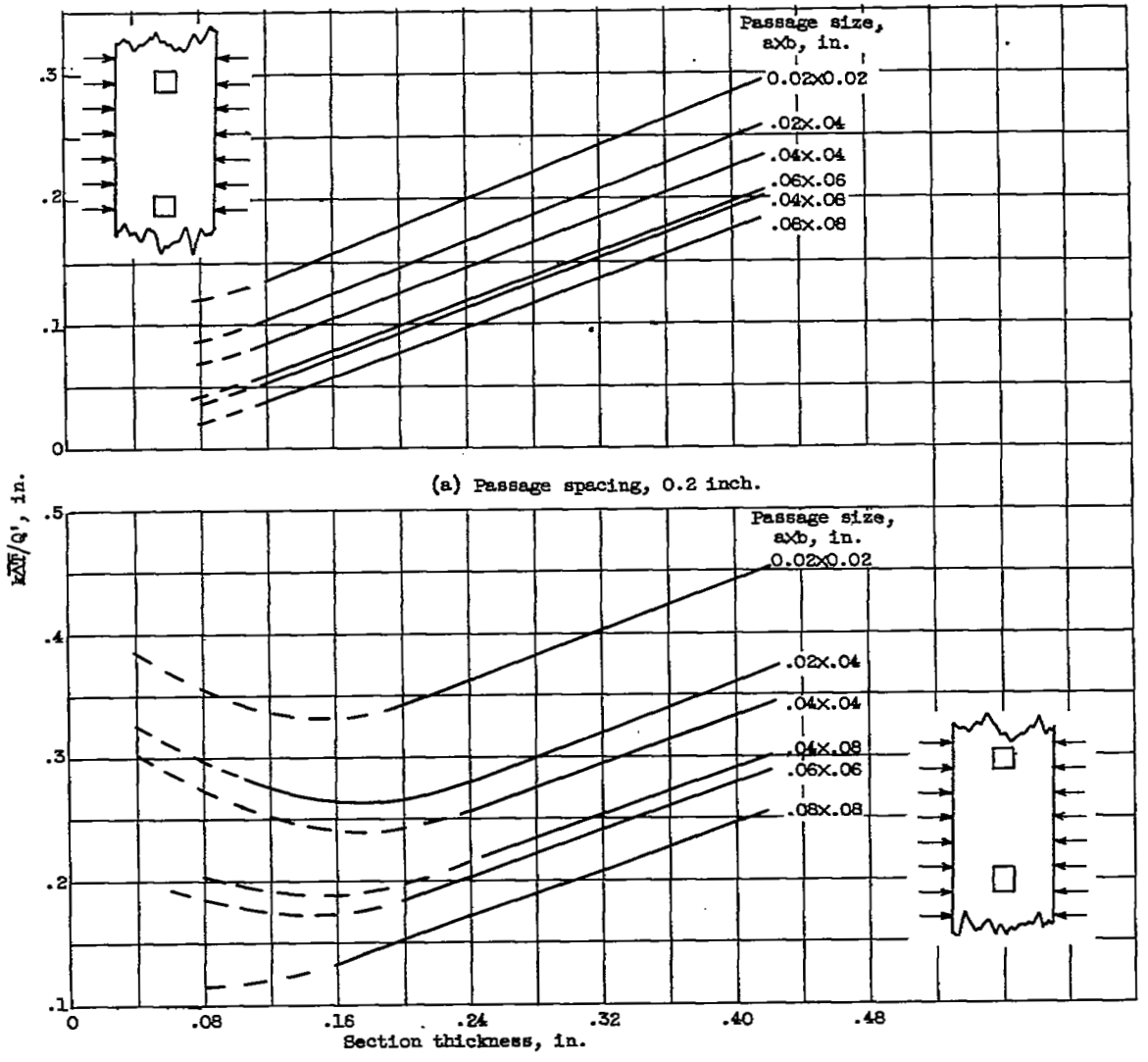

Figure 7. - Variation of $k\overline{\Delta T}/Q'$ with section thickness in sections heated on two opposing sides.

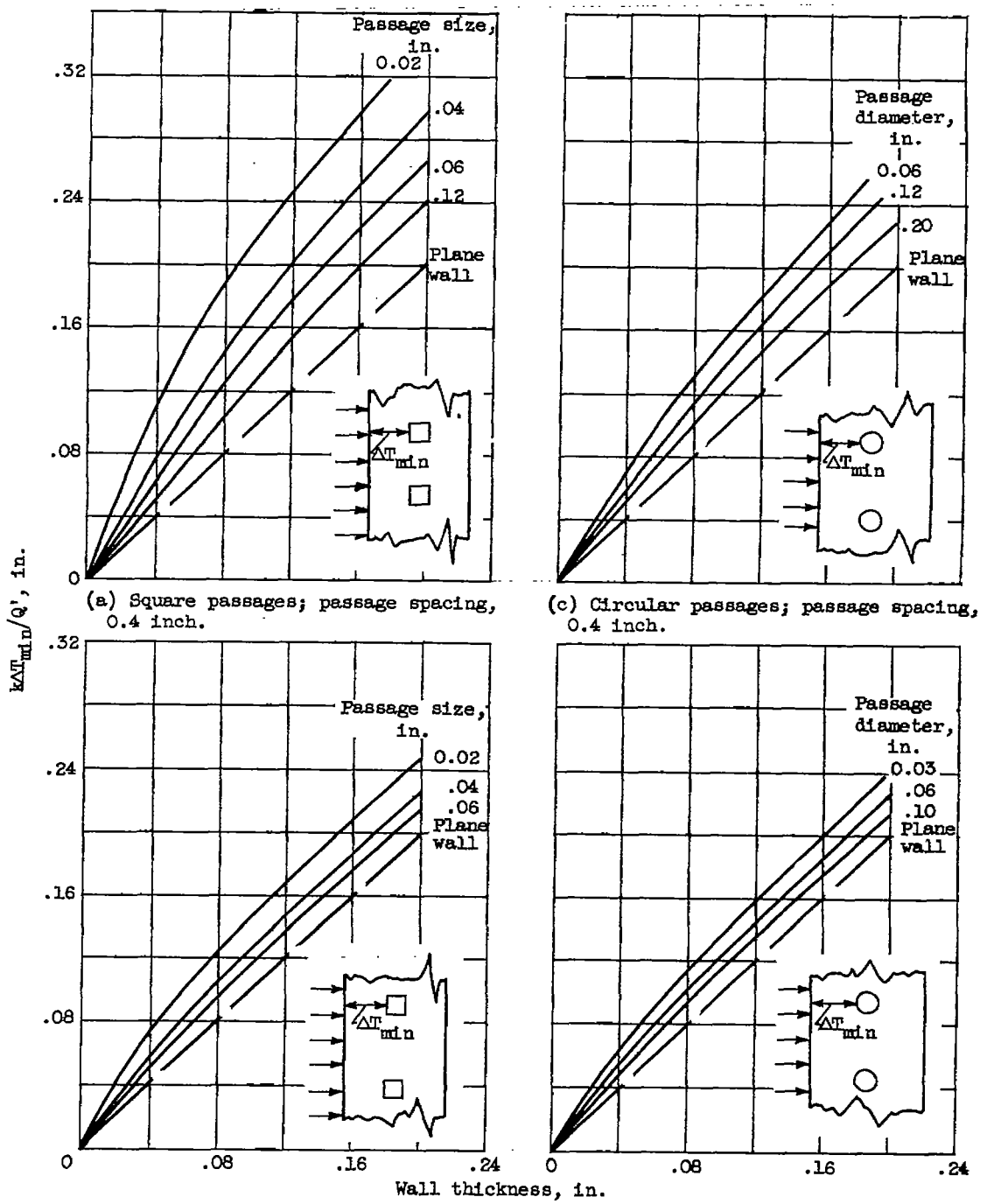

(a) Square passages; passage spacing, 0.4 inch.

(c) Circular passages; passage spacing, 0.4 inch.

(b) Square passages; passage spacing, 0.2 inch.

(d) Circular passages; passage spacing, 0.2 inch.

Figure 8. - Variation of $k\Delta T_{min}/Q'$ with wall thickness for square and circular passages in section whose depth is large with respect to passage dimensions.

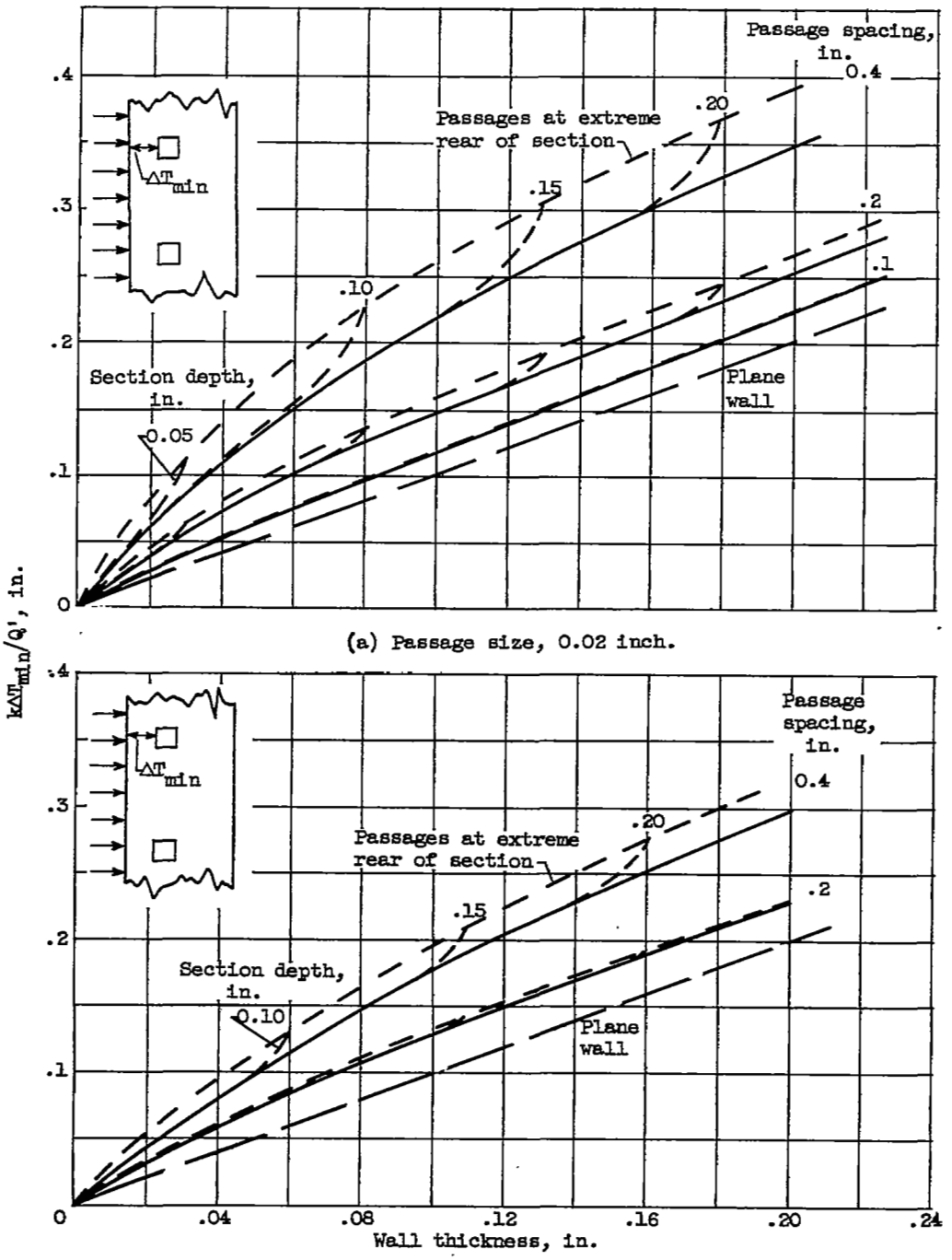

(a) Passage size, 0.02 inch.

(b) Passage size, 0.04 inch.

Figure 9. - Variation of $k\Delta T_{min}/Q'$ with wall thickness in sections of various depths. Square passages.

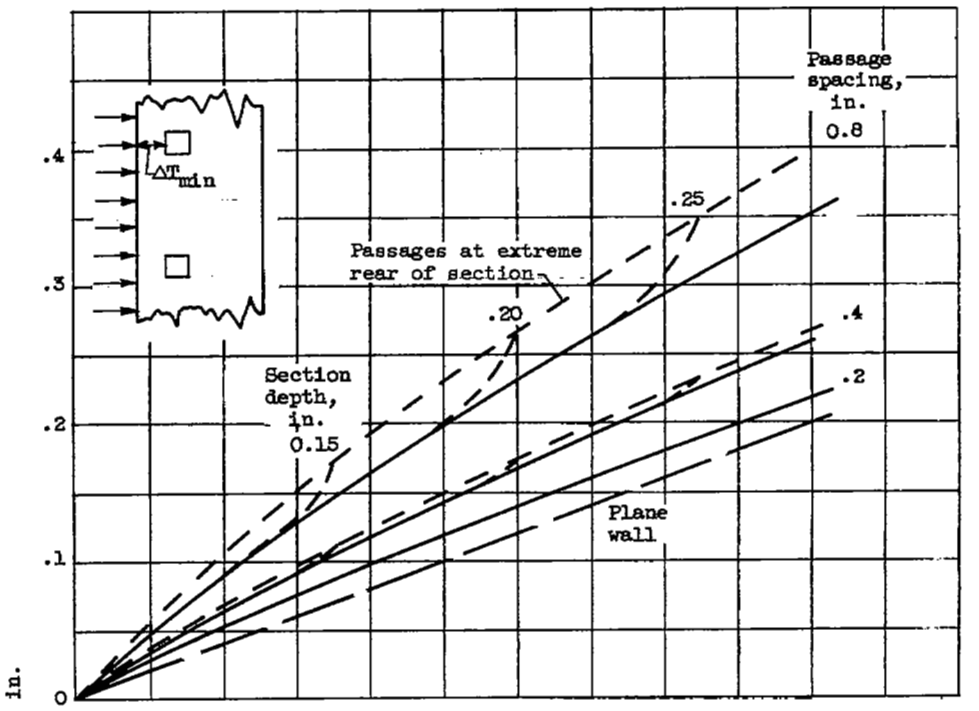

(c) Passage size, 0.08 inch.

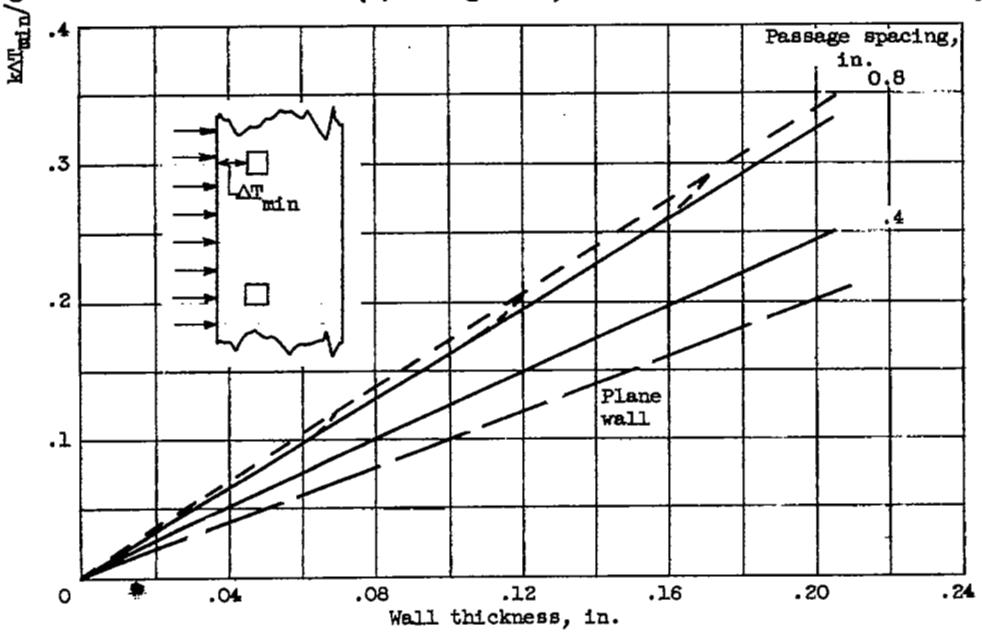

(d) Passage size, 0.12 inch.

Figure 9. - Concluded. Variation of $k\Delta T_{min}/Q'$ with wall thickness in sections of various depths. Square passages.

[redacted]

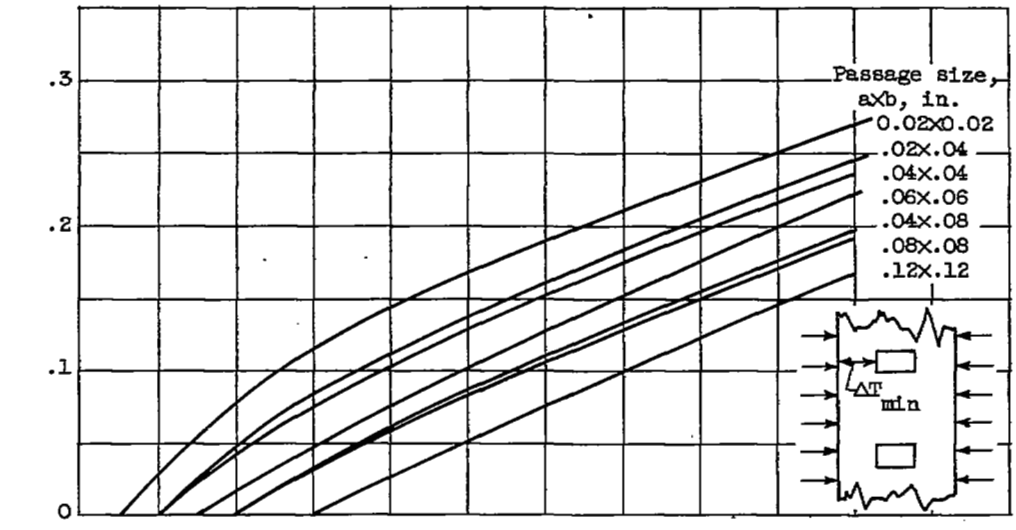

(a) Passage spacing, 0.2 inch.

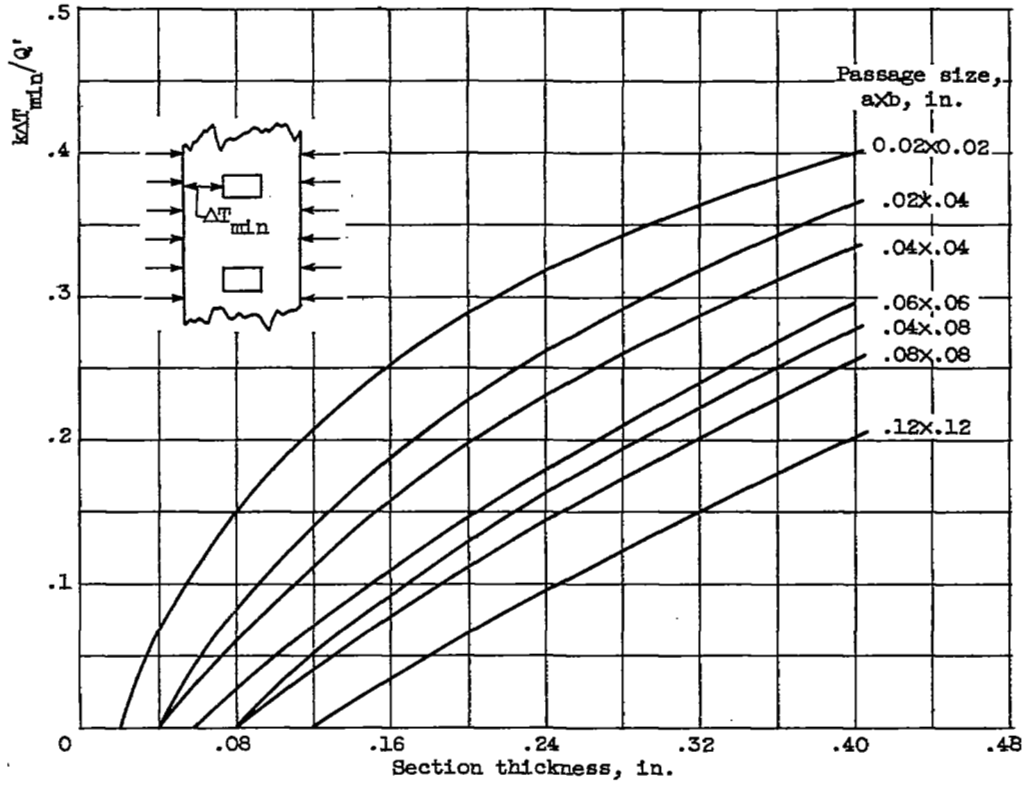

(b) Passage spacing, 0.4 inch.

Figure 10. - Variation of $k\Delta T_{min}/Q'$ with section thickness in sections heated on two opposing sides.

[redacted]

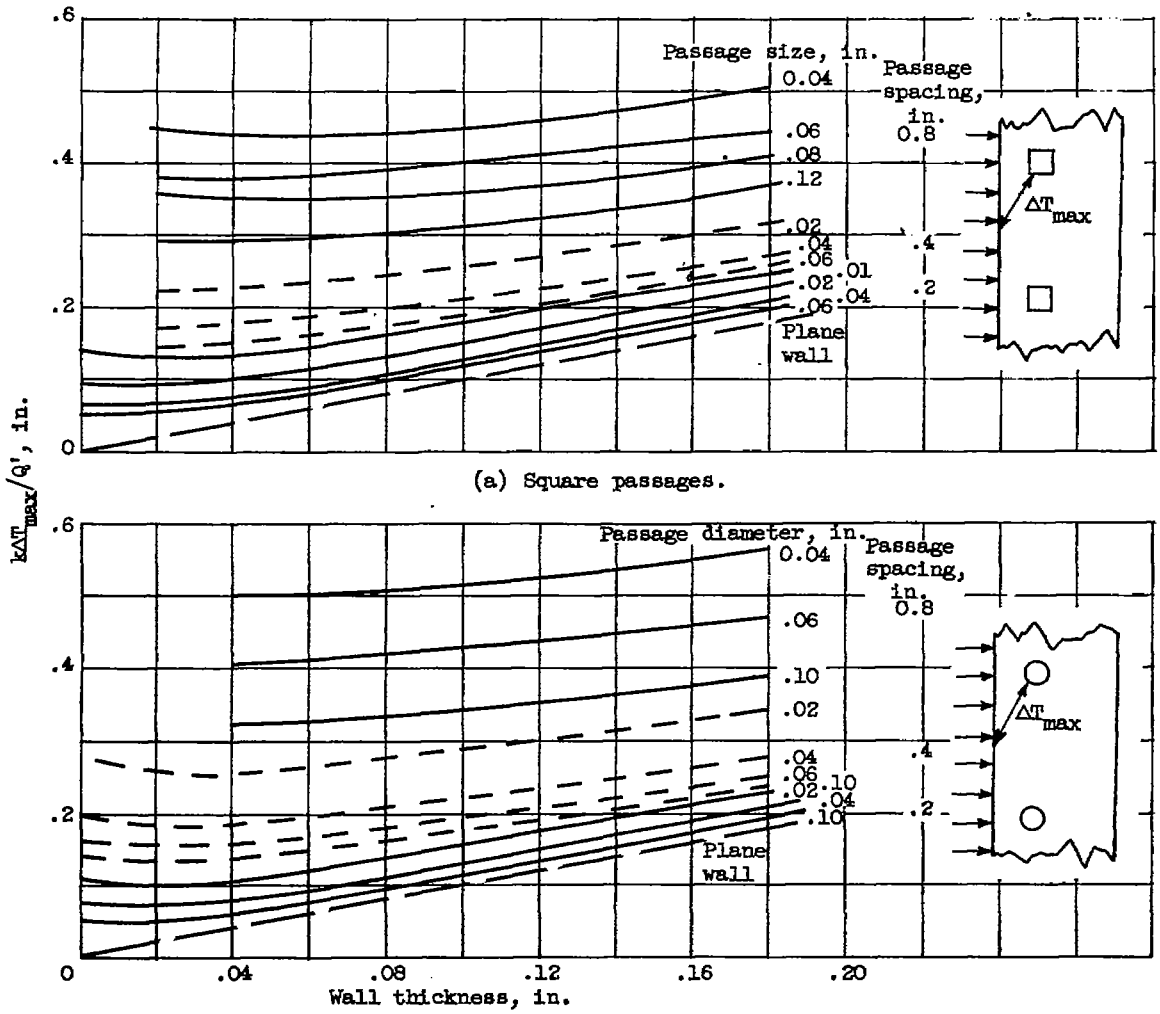

(a) Square passages.

(b) Circular passages.

Figure 11. - Variation of $k\Delta T_{max}/Q'$ with wall thickness in section whose depth is large with respect to passage dimensions.

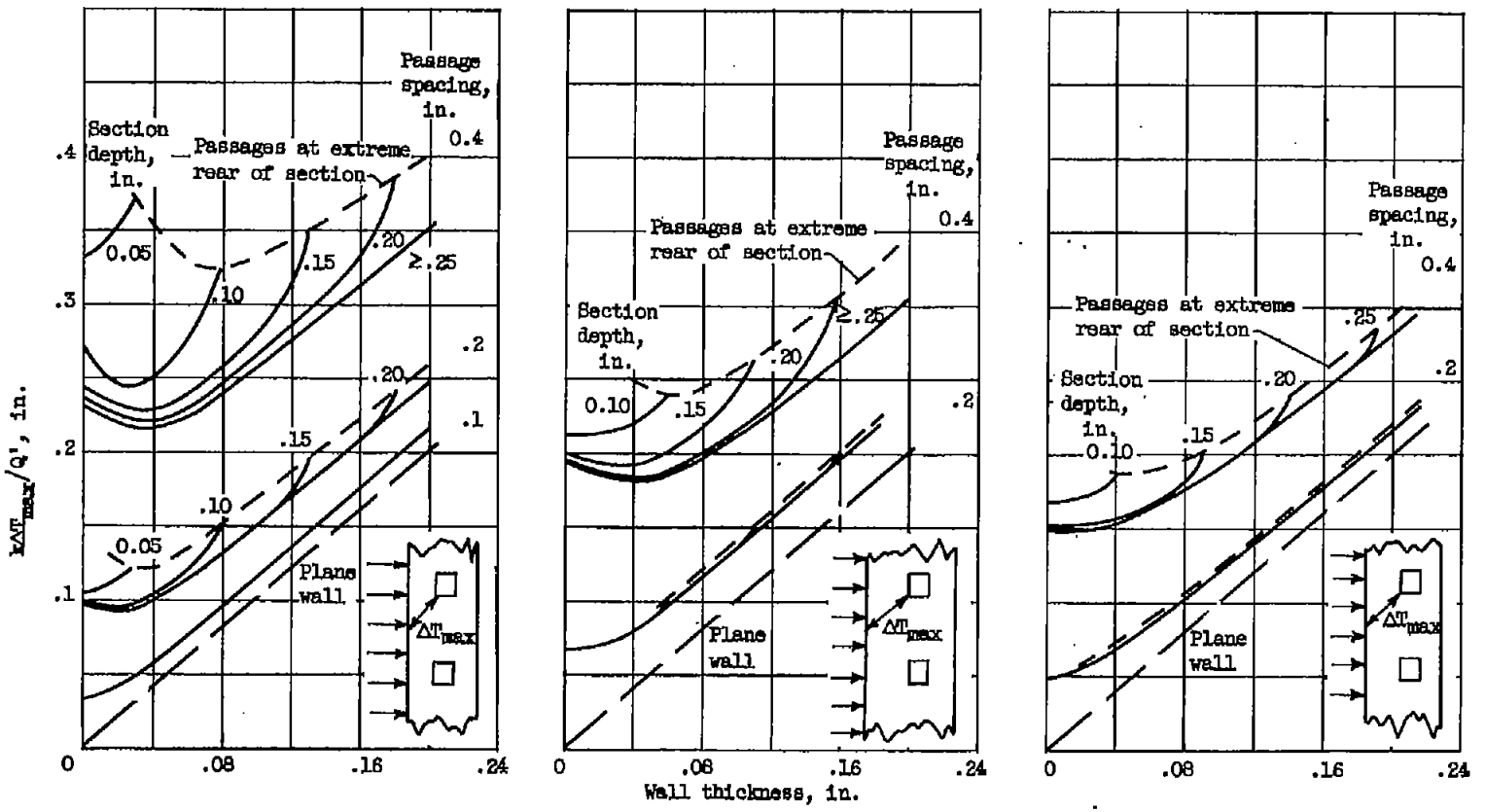

(a) Passage size, 0.02 inch. (b) Passage size, 0.04 inch. (c) Passage size, 0.06 inch.

Figure 12. - Variation of $k\Delta T_{max}/Q'$ with wall thickness for various section depths and passage spacings. Square passages.

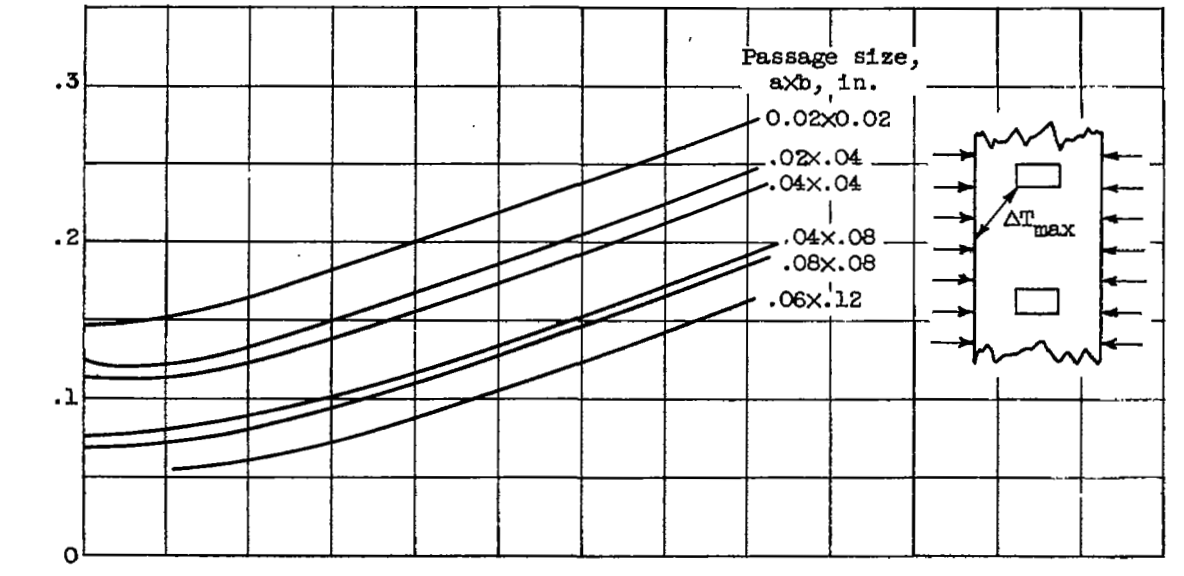

(a) Passage spacing, 0.2 inch.

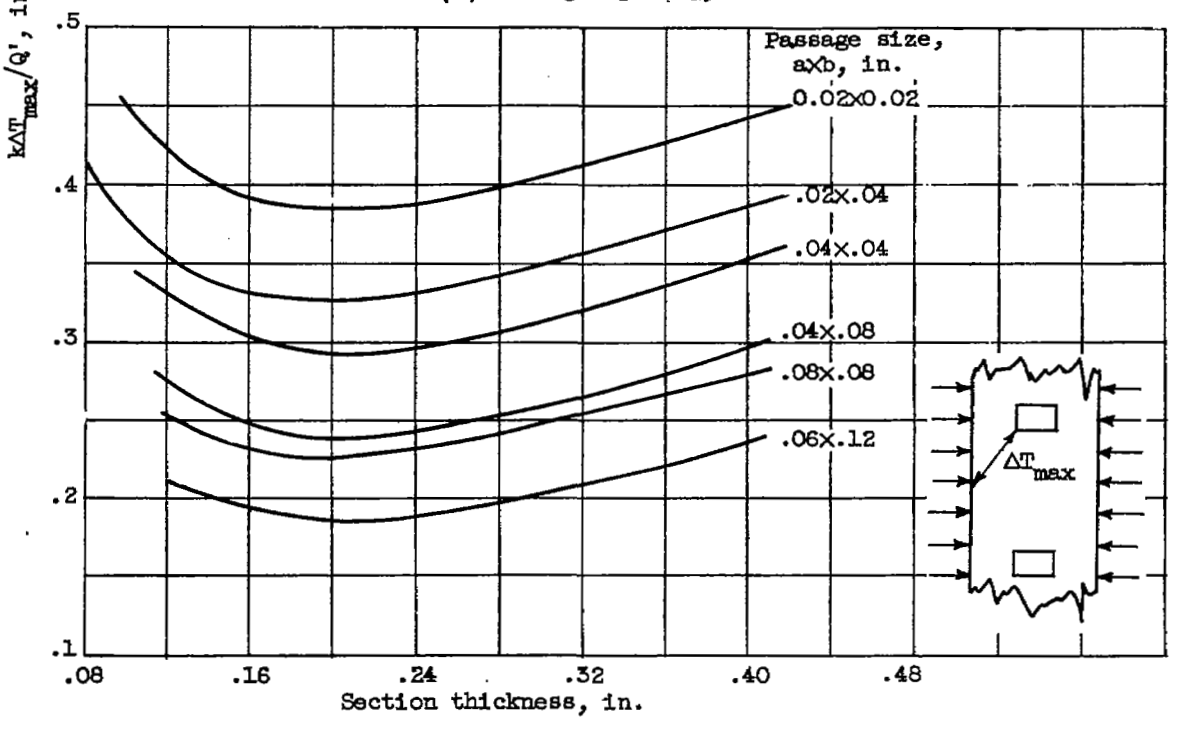

(b) Passage spacing, 0.4 inch.

Figure 13. - Variation of $k\Delta T_{max}/Q'$ with section thickness in sections heated on two opposing sides.

[redacted]

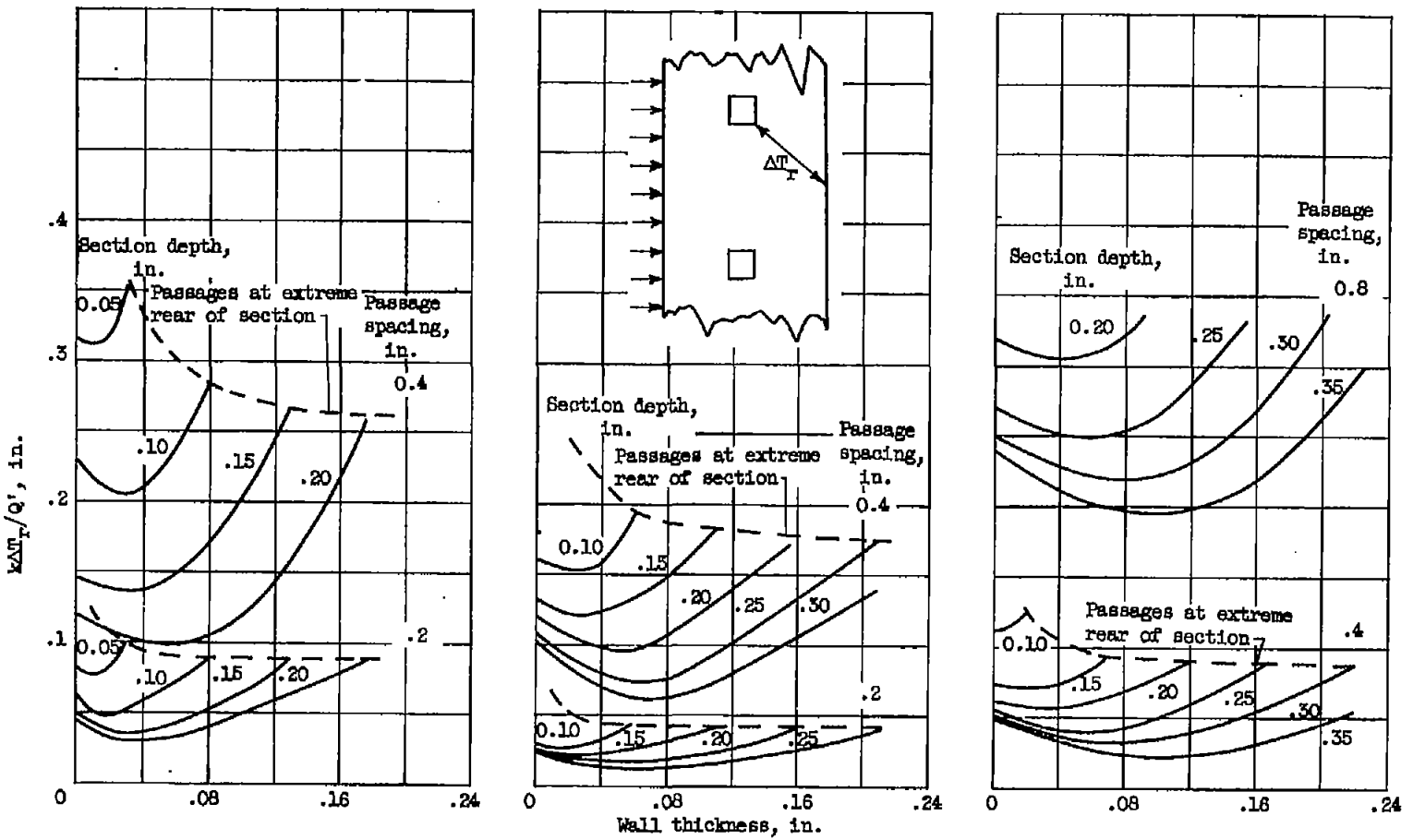

(a) Passage size, 0.02 inch. (b) Passage size, 0.04 inch. (c) Passage size, 0.08 inch.

Figure 14. - Variation of $k\Delta T_r/Q'$ with wall thickness for various section depths and passage spacings. Square passages.

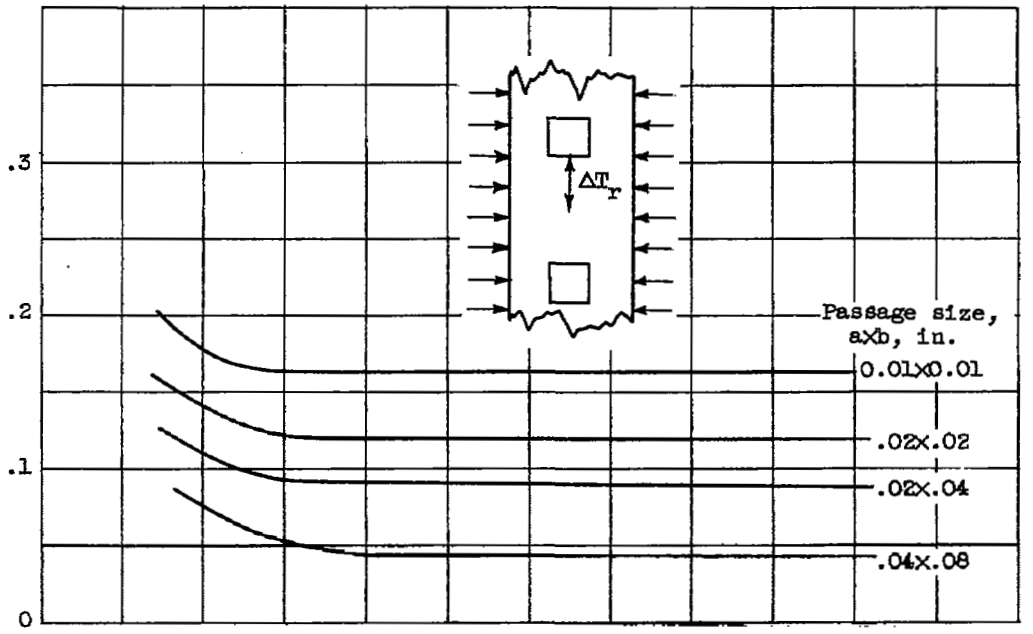

(a) Passage spacing, 0.2 inch.

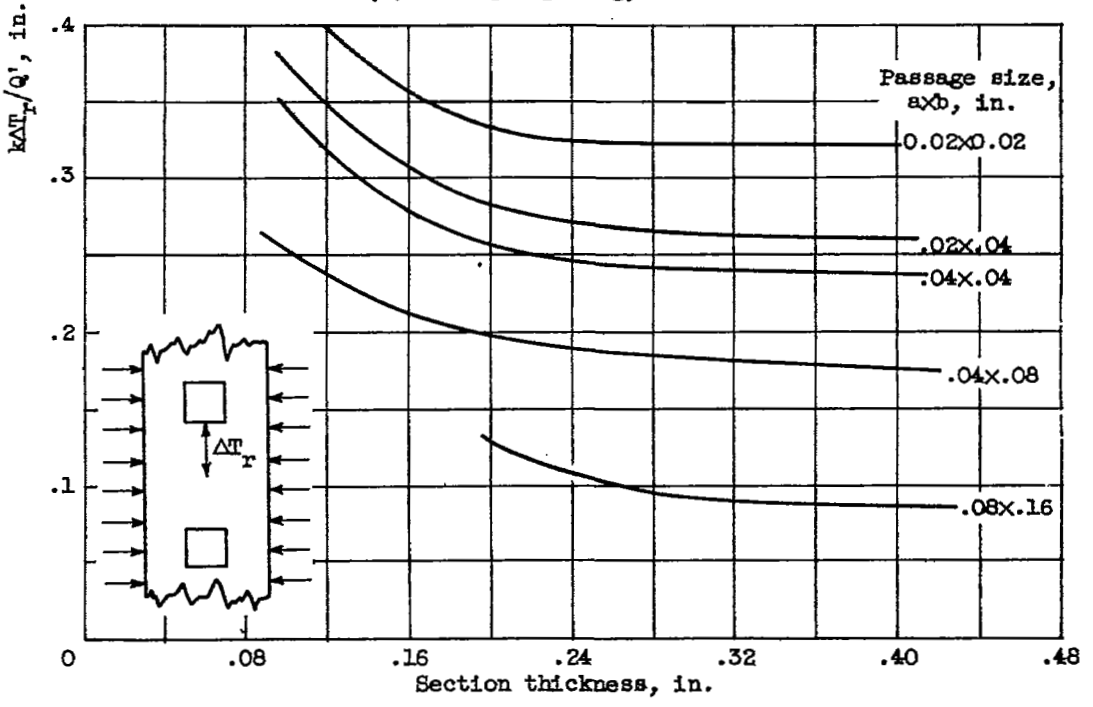

(b) Passage spacing, 0.4 inch.

Figure 15. - Variation of $k\Delta T_r/Q'$ with section thickness in sections heated on two opposing sides.